

Generalized Langevin dynamics for single beads in linear elastic network

Soya Shinkai,¹ Shuichi Onami,¹ and Tomoshige Miyaguchi^{2,*}

¹*Laboratory for Developmental Dynamics, RIKEN Center for Biosystems Dynamics Research, Kobe 650-0047, Japan*

²*Department of Systems Engineering, Wakayama University, 930 Sakaedani, Wakayama 640-8510, Japan*

(Dated: October 23, 2024)

We derive generalized Langevin equations (GLEs) for single beads in linear elastic networks. In particular, the derivations of the GLEs are conducted without employing normal modes, resulting in two distinct representations in terms of resistance and mobility kernels. The fluctuation-dissipation relations are also confirmed for both GLEs. Subsequently, we demonstrate that these two representations are interconnected via Laplace transforms. Furthermore, another GLE is derived by utilizing a projection operator method, and it is shown that the equation obtained through the projection scheme is consistent with the GLE with the resistance kernel. As simple examples, the general theory is applied to the Rouse model and the ring polymer, where the GLEs with the resistance and mobility kernels are explicitly derived for arbitrary positions of the tagged bead in these models. Finally, the GLE with the mobility kernel is also derived for the elastic network with hydrodynamic interactions under the pre-averaging approximation.

I. INTRODUCTION

Not only do macromolecules such as proteins diffuse in solutions, but components comprising the macromolecules, such as monomers and amino acids (referred to as beads hereafter), also exhibit time-dependent fluctuations. To describe such internal motion of macromolecules, elastic network models have been widely employed [1–6]. Beads in the elastic networks are connected by Hookean springs. The simplest example of such models is the ideal Rouse chain [7, 8], but the elastic network models also include polymers with network structures, in which a bead can be linked to more than two beads. Polymers with such network structures, forming branches and crosslinks, are also considered important for modeling three-dimensional genome structures [9–12].

Experimental studies have revealed complex properties in single beads dynamics, and therefore, elucidating equations of motion that can describe such intricate behaviors of single beads is essential for analyzing experimental data. For instance, motions of single nucleosomes and single genomic loci within chromatin fibers exhibit subdiffusion [13–18]. Furthermore, by indirectly monitoring distance fluctuations between a pair of beads in a protein, it was reported that these fluctuations can be described by a generalized Langevin equation (GLE) [19, 20].

In theoretical studies, it was demonstrated that single beads dynamics of a linear chain, such as the Rouse model, can be described by GLEs, as analytically proven in Refs. [21–27] by using normal modes. For instance, in Refs. [21, 22, 24], it was shown that the middle bead of the Rouse and other linear polymer models follows a GLE with a resistance memory kernel. Meanwhile, in Refs. [25, 26], a tagged bead in the linear chains was shown to follow a GLE with a mobility memory kernel,

regardless of the position of the tagged bead in the chain. However, a derivation of the GLEs for bead motions in the elastic network model has not been undertaken.

To the best of the authors' knowledge, the derivations of the GLEs for polymer models have relied on normal mode techniques [21, 22, 24, 25]. Contrastingly, in the projection operator formalism, a slightly different form of the GLE is derived [28, 29] without relying on the normal modes. Considering that the derivations of the GLEs in linear polymer models can be viewed as a concrete example of the projection operator formalism [22], it is anticipated that the GLEs for the polymer models and the elastic networks can be derived without resorting to the normal modes. The derivations of the GLEs in linear polymer models were carried out by eliminating modes other than the tagged bead from the equations of motion [21, 22, 24, 25]. However, it has remained unclear how such procedures are related to the projection operator scheme.

In this paper, we show that single-bead motion of the linear elastic networks can be described by the GLEs. We utilize supervector notation [29], which plays a crucial role in the derivations of the GLEs. In a projection operator analysis, we employ the Hermitian conjugate of the Smoluchowski operator [29]. After deriving the GLEs, normal-mode equations of motion are constructed with careful attention to preserving translational symmetry in space. Numerical simulations are carried out to validate theoretical results for the Rouse model. Hydrodynamic interactions (HIs) are incorporated into the model through a preaveraged mobility tensor [8].

Firstly, we derive two GLEs for bead motion in linear elastic network models, one with a resistance kernel and the other with a mobility kernel. In particular, both GLEs are derived without resorting to normal modes. Secondly, another GLE is derived using the projection operator method, and it is demonstrated that this third GLE is consistent with the GLE with the resistance kernel, although they are not equivalent. Since normal modes are not used in these derivations, the correspon-

* mygch@wakayama-u.ac.jp

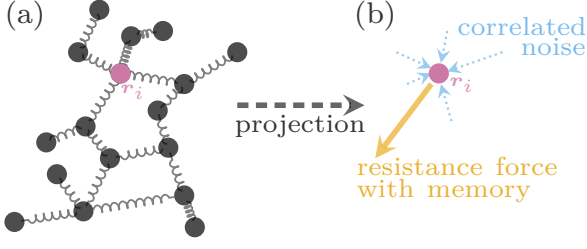


FIG. 1. (a) Schematic illustration of the elastic network model. The circles and springs represent beads and harmonic interactions, respectively. These harmonic interactions are defined by the matrix L in Eq. (3). (b) By projecting out the beads \mathbf{r}_j other than the tagged one \mathbf{r}_i , we derive the GLE with the resistance kernel [Eq. (17)]. In the GLE, the interactions with the other beads \mathbf{r}_j are divided into two components: a resistance force with memory (solid arrow) and a correlated noise (dotted arrows).

dence between these GLEs becomes clear. Thirdly, by using normal modes, we derive diagonalized GLEs with the resistance and mobility kernels, and directly demonstrate that these GLEs are interconnected via Laplace transforms. Fourthly, the present framework is applied to the ideal Rouse model, revealing that the memory kernels vary slightly depending on the locations of the tagged bead in the Rouse chain. Finally, the GLE with the mobility kernel is derived for the system with the HI.

This paper is organized as follows. In Sec. II, we introduce the linear elastic network and the supervector notation. In Sec. III, the three GLEs are derived for single-bead motion in the linear elastic network. Additionally, the fluctuation-dissipation relations (FDRs) are confirmed in this section. In Sec. IV, the normal modes are introduced, and the memory kernels and correlated noises are represented with these modes. In Sec. V, the present framework is applied to single-bead dynamics of simple polymer models: the Rouse model and the ring polymer. In Sec. VI, for the linear elastic network with the HI, the GLE with the mobility kernel is derived. Section VII is devoted to a discussion.

II. MODEL

In this section, we introduce the linear elastic network, which is then represented with the supervector notation. In addition, reduced vectors and matrices are defined; they play a crucial role in derivations of the GLEs.

A. Linear elastic network

We study a linear elastic network model with N beads, illustrated in Fig. 1(a). This model is described by the

Langevin equation [8, 29] as

$$\gamma \frac{d\mathbf{r}_m(t)}{dt} = \sum_{n=1}^N k_{mn}[\mathbf{r}_n(t) - \mathbf{r}_m(t)] + \boldsymbol{\xi}_m(t), \quad (1)$$

with $m = 1, \dots, N$. Here, $\mathbf{r}_m(t)$ is the position vector of the m th bead, and γ is a friction constant. Moreover, $\boldsymbol{\xi}_m(t)$ is a three-dimensional Gaussian white noise; if the system is in equilibrium, $\boldsymbol{\xi}_m(t)$ should satisfy the FDR

$$\langle \boldsymbol{\xi}_m(t_1) \boldsymbol{\xi}_n(t_2) \rangle = 2k_B T \gamma \delta(t_1 - t_2) \delta_{mn} I_3. \quad (2)$$

Here k_B is the Boltzmann constant, T is the absolute temperature, I_n is the $n \times n$ identity tensor, $\delta(t)$ is the delta function, and δ_{mn} is the Kronecker delta. In this paper, we neglect the excluded volume effect, whereas the HI is incorporated in the subsection after next.

In addition, k_{mn} in Eq. (1) represents a spring constant between the m th and n th beads; it is assumed that k_{mn} is symmetric, i.e., $k_{mn} = k_{nm}$, and that the diagonal entries are zero, $k_{nn} = 0$. For physical modeling of three-dimensional genome data, it is important to accommodate the possibility of some spring constants being negative [12]. Consequently, instead of assuming $k_{mn} \geq 0$, we only require that one eigenvalue of the Kirchhoff matrix L , which is defined below, is zero, while the remaining $N - 1$ eigenvalues are positive to ensure thermodynamic stability. This allows for the possibility of some k_{mn} being negative. Thus, the present model is termed a linear elastic network with non-negative eigenvalues.

We define an $N \times N$ matrix L by $(L)_{mn} := l_{mn}$, where $l_{mn} := \delta_{mn} d_n - k_{mn}$ with $d_n := \sum_{m=1}^N k_{mn}$. Note that L is symmetric, $l_{mn} = l_{nm}$. Moreover, we employ supervector notation $\mathbf{r} := (\mathbf{r}_1, \dots, \mathbf{r}_N)$ and $\boldsymbol{\xi} := (\boldsymbol{\xi}_1, \dots, \boldsymbol{\xi}_N)$. Then, Eq. (1) is rewritten as [7]

$$\gamma \frac{d\mathbf{r}(t)}{dt} = -L \cdot \mathbf{r}(t) + \boldsymbol{\xi}(t), \quad (3)$$

where the dot symbol represents the inner product of a (super)matrix and a (super)vector. We also use the dot symbol to denote the inner product of two (super)vectors, as in $\mathbf{v} \cdot \mathbf{w}$. In this notation, it is irrelevant whether a vector is a column or a row vector [Exceptions are vectors used in block matrices, such as in Eqs. (8), (30) and (31), where we distinguish between row and column vectors with a transpose sign. See details below]. For example, the expression $\mathbf{v}^t A \mathbf{w}$ in matrix notation can be simply written as $\mathbf{v} \cdot A \cdot \mathbf{w}$. In contrast, $\mathbf{v} \mathbf{w}$ represents the tensor product of two vectors, resulting in a rank-two tensor.

An inner product (contraction) of two (super)matrices, say A and B , is denoted simply as AB . This notation is unambiguous, because tensor products of matrices of the same size do not appear in this article.

With the supervector notation, the FDR in Eq. (2) is expressed as

$$\langle \boldsymbol{\xi}(t_1) \boldsymbol{\xi}(t_2) \rangle = 2k_B T \gamma \delta(t_1 - t_2) I_3 I_N, \quad (4)$$

where $I_3 I_N$ should be understood as an $N \times N$ matrix, with the (i, j) element being $I_3 \delta_{ij}$ (In other words, I_3 should be treated as if it is a scalar). In some literature, $I_3 I_N$ is denoted as $I_3 \otimes I_N$ [3], but here we employ the brief notation.

Note that the matrix elements l_{mn} of L satisfy

$$\sum_{n=1}^N l_{mn} = 0 \quad (m = 1, \dots, N), \quad (5)$$

which is a manifestation of translational symmetry. From Eq. (5), it follows that L has a zero eigenvalue with the associated eigenvector $\mathbf{1}_N := (1, \dots, 1)$, i.e., $L \cdot \mathbf{1}_N = 0$. As stated above, we assume that one eigenvalue of L is zero and the remaining $N - 1$ eigenvalues are positive, i.e., L is positive semidefinite.

B. Reduced vector and matrix

We designate the i th bead as the tagged bead, and derive equations describing its dynamics in the subsequent section. To accomplish this, we introduce an operation, which is closely related to the projection operation. For an N -dimensional vector $\mathbf{u} = (u_1, \dots, u_N)$ and an N -dimensional supervector $\mathbf{w} = (\mathbf{w}_1, \dots, \mathbf{w}_N)$, we define $(N - 1)$ -dimensional vector \mathbf{u}' and supervector \mathbf{w}' as

$$\mathbf{u}' = (u_1, \dots, u_{i-1}, u_{i+1}, \dots, u_N), \quad (6)$$

$$\mathbf{w}' = (\mathbf{w}_1, \dots, \mathbf{w}_{i-1}, \mathbf{w}_{i+1}, \dots, \mathbf{w}_N). \quad (7)$$

Similarly, we define a reduced matrix L' of order $N - 1$ by eliminating the i th row and column from L . More precisely, let us express the matrix L as $L = [\mathbf{l}_1, \dots, \mathbf{l}_N]$, where \mathbf{l}_j is a column vector corresponding to the j th column of L . Note also that we use the square brackets to denote a matrix, thereby distinguishing it from a supervector. Then L' can be written by

$$L' = [\mathbf{l}'_1, \dots, \mathbf{l}'_{i-1}, \mathbf{l}'_{i+1}, \dots, \mathbf{l}'_N]. \quad (8)$$

In block matrices, such as in Eq. (8), vectors with a transpose sign are always considered row vectors, while those without the sign are considered column vectors [See Eqs. (30) and (31)]. The prime represents an operation of dimensionality reduction of vectors and matrices.

It may be worth noting a connection to the projection operator formalism here. In that formalism, a projection \mathcal{P} onto a slow variable is introduced, and \mathcal{Q} is also defined as a complementary projection satisfying $\mathcal{P} + \mathcal{Q} = \mathcal{I}$ with \mathcal{I} being the identity operator. As demonstrated in Sec. III D, the reduction of L to L' is related to the action of \mathcal{Q} to the Hermitian conjugate of the Smoluchowski operator \mathcal{L}_S^\dagger [See Eq. (55)].

By using these vectors and matrices, Eq. (5) can be rewritten as $\sum_{n=1}^N \mathbf{l}'_n = 0$, or equivalently

$$\mathbf{l}'_i = - \sum_{n=1, n \neq i}^N \mathbf{l}'_n = -L' \cdot \mathbf{1}. \quad (9)$$

Here, $\mathbf{1}$ represents an $N - 1$ dimensional vector with all elements being unity, i.e., $\mathbf{1} =: (1, \dots, 1)$. It is important to note that L' is also a symmetric matrix and is positive definite (See Appendix A).

Utilizing the relation $L \cdot \mathbf{r} = \mathbf{r}_1 \mathbf{l}_1 + \dots + \mathbf{r}_N \mathbf{l}_N$ and Eq. (9), we obtain

$$(L \cdot \mathbf{r})' = L' \cdot \mathbf{r}' + \mathbf{r}_i \mathbf{l}'_i = L' \cdot (\mathbf{r}' - \mathbf{r}_i \mathbf{1}). \quad (10)$$

Again, note that $\mathbf{r}_i \mathbf{l}'_i$ should be regarded as a supervector, each element of which is given by $\mathbf{r}_i \mathbf{l}_{ji}$, i.e., \mathbf{r}_i should be treated as if it is a scalar. Similarly, $\mathbf{r}_i \mathbf{1}$ is a supervector, with each element being \mathbf{r}_i .

C. Hydrodynamic interaction

If we take into account the HI with pre-averaging approximation [8], the equation of motion [Eq. (3)] is rewritten as

$$\frac{d\mathbf{r}(t)}{dt} = -L_H \cdot \mathbf{r}(t) + \boldsymbol{\xi}_H(t), \quad (11)$$

with $L_H := HL$ and $\boldsymbol{\xi}_H = H \cdot \boldsymbol{\xi}$, where H is the pre-averaged motility matrix (an $n \times n$ non-singular matrix independent of t). The noise vector $\boldsymbol{\xi}_H$ satisfies the FDR [8, Sec.3.3]

$$\langle \boldsymbol{\xi}_H(t_1) \boldsymbol{\xi}_H(t_2) \rangle = 2k_B T \delta(t_1 - t_2) I_3 H. \quad (12)$$

If the HI is absent, H is a diagonal matrix, resulting in an elastic network with beads of different masses [30]. In particular, when $H = \mathbf{I}_N / \gamma$, Eqs. (11) and (12) reduce to Eqs. (3) and (4), respectively.

It can be readily shown that Eq. (10) also holds for L_H :

$$(L_H \cdot \mathbf{r})' = L'_H \cdot (\mathbf{r}' - \mathbf{r}_i \mathbf{1}). \quad (13)$$

Note that while L is symmetric, L_H is not. Therefore, $\mathbf{1}$ is the right eigenvector of L_H with a zero eigenvalue, but it is not necessarily the left eigenvector. However, L_H has a left eigenvector \mathbf{w} with a zero eigenvalue. Because H is non-singular, $\mathbf{w} \cdot H = \mathbf{1}$ if the zero mode \mathbf{w} is suitably normalized. We assume that the i th entry of \mathbf{w} , w_i , is not zero: $w_i \neq 0$.

III. DERIVATION OF THREE GLES

It is well-known that memory effects in GLEs can be characterized either by resistance (friction) or mobility [31]. In this section, we derive two GLEs: one with the resistance kernel and the other with the mobility kernel. The interrelation of these two representations will be discussed in Secs. III C and IV D. Additionally, using a projection operator scheme, we also derive another GLE.

A. GLE with resistance kernel

By applying the prime operator to Eq. (3), the equations of motion for the beads \mathbf{r}_m ($m \neq i$) are given by

$$\gamma \frac{d\mathbf{r}'(t)}{dt} = -L' \cdot [\mathbf{r}'(t) - \mathbf{r}_i(t)\mathbf{1}] + \boldsymbol{\xi}'(t), \quad (14)$$

where Eq. (10) is used. From Eq. (1), the equation of motion for the i th bead is given by

$$\begin{aligned} \gamma \frac{d\mathbf{r}_i(t)}{dt} &= \sum_{n=1}^N k_{in}[\mathbf{r}_n(t) - \mathbf{r}_i(t)] + \boldsymbol{\xi}_i(t) \\ &= \mathbf{1} \cdot L' \cdot [\mathbf{r}'(t) - \mathbf{r}_i(t)\mathbf{1}] + \boldsymbol{\xi}_i(t), \end{aligned} \quad (15)$$

where we used the fact that $k_{in} = -l_{in}$ if $n \neq i$ and Eq. (9). Now, the translational symmetry of the system is clearly discernible in Eqs. (14) and (15).

A formal solution of Eq. (14) is given by

$$\begin{aligned} \mathbf{r}'(t) - \mathbf{r}_i(t)\mathbf{1} &= - \int_0^t e^{-\frac{L'}{\gamma}(t-\tau)} \cdot \mathbf{1} \dot{\mathbf{r}}_i(\tau) d\tau \\ &+ \frac{1}{\gamma} \int_0^t e^{-\frac{L'}{\gamma}(t-\tau)} \cdot \boldsymbol{\xi}'(\tau) d\tau + e^{-\frac{L'}{\gamma}t} \cdot \delta\mathbf{r}'(0), \end{aligned} \quad (16)$$

where integration by parts is used to obtain the first term on the right-hand side, and $\delta\mathbf{r}'(0)$ is defined by $\delta\mathbf{r}'(0) := \mathbf{r}'(0) - \mathbf{r}_i(0)\mathbf{1}$. We also utilized the fact that the order of multiplications between vectors and symmetric matrices, such as $e^{-L't/\gamma}$, is immaterial.

Inserting Eq. (16) into Eq. (15), we obtain a GLE

$$\gamma \frac{d\mathbf{r}_i(t)}{dt} + \gamma \int_0^t \mu(t-\tau) \dot{\mathbf{r}}_i(\tau) d\tau = \boldsymbol{\xi}_i(t) + \boldsymbol{\xi}_i^r(t), \quad (17)$$

where $\mu(t)$ is a memory kernel and $\boldsymbol{\xi}_i^r(t)$ is a colored noise defined respectively as

$$\gamma\mu(t) := \mathbf{1} \cdot L' e^{-\frac{L'}{\gamma}t} \cdot \mathbf{1}, \quad (18)$$

$$\boldsymbol{\xi}_i^r(t) := \mathbf{1} \cdot L' \cdot \left[\frac{1}{\gamma} \int_0^t e^{-\frac{L'}{\gamma}(t-\tau)} \cdot \boldsymbol{\xi}'(\tau) d\tau + e^{-\frac{L'}{\gamma}t} \cdot \delta\mathbf{r}'(0) \right]. \quad (19)$$

Thus, the interaction forces exerted on the tagged bead by the other beads are divided into the resistance force with memory and the colored noise as illustrated in Fig. 1(b). Therefore, the memory kernel $\gamma\mu(t)$ is referred to as a resistance kernel. We place γ in front of the second term in the left-hand side of Eq. (17) to render the Laplace transform of $\mu(t)$ dimensionless. Note also that the two noise terms, the white noise $\boldsymbol{\xi}_i(t)$ and the colored noise $\boldsymbol{\xi}_i^r(t)$, are mutually independent.

Equation (17) is an overdamped version of the GLE. This type of GLE was originally derived in Ref. [22] for single-bead motion in linear polymer models by using normal modes. Here, we derive the same equation for a general setting without relying on normal modes. It is

also noteworthy that Eq. (17) with any resistance kernel $\mu(t)$ can be numerically integrated by using a Markov embedding method proposed in Ref. [32].

Now, let us show that Eqs. (18) and (19) satisfy the FDR. From Eq. (4), $\boldsymbol{\xi}'(t)$ satisfies the FDR

$$\langle \boldsymbol{\xi}'(t_1) \boldsymbol{\xi}'(t_2) \rangle = 2k_B T \gamma \delta(t_1 - t_2) I_3 I_{N-1}. \quad (20)$$

Moreover, if we assume that $\mathbf{r}'(t)$ is in equilibrium at $t = 0$, then $\delta\mathbf{r}'(0)$ follows the canonical distribution

$$\propto \exp \left[-\frac{\delta\mathbf{r}'(0) \cdot L' I_3 \cdot \delta\mathbf{r}'(0)}{2k_B T} \right], \quad (21)$$

where $\delta\mathbf{r}' \cdot L' I_3 \cdot \delta\mathbf{r}'/2$ is the potential energy [See also Eq. (14)]. In Eq. (21), the dot products should be understood as $3(N-1)$ -dimensional contractions. Therefore, the covariant matrix of $\delta\mathbf{r}'(0)$ is given by

$$\langle \delta\mathbf{r}'(0) \delta\mathbf{r}'(0) \rangle = k_B T L'^{-1} I_3. \quad (22)$$

Note that the inversion L'^{-1} exists because L' is positive definite [See Appendix A]. From Eqs. (19), (20) and (22), the FDR is readily obtained as

$$\langle \boldsymbol{\xi}_i^r(t_1) \boldsymbol{\xi}_i^r(t_2) \rangle = \gamma k_B T I_3 \mu(t_1 - t_2). \quad (23)$$

B. GLE with mobility kernel

Next, to derive a GLE with the mobility-kernel representation [25], let us introduce an external force $\mathbf{f}_{\text{ex}}(t)$ exerted on the tagged bead i . We assume that the external force $\mathbf{f}_{\text{ex}}(t)$ is switched on at $t = 0$ at which the system is in equilibrium. The equation of motion is then written as

$$\gamma \frac{d\mathbf{r}(t)}{dt} = -L \cdot \mathbf{r}(t) + \mathbf{f}_{\text{ex}}(t) \mathbf{e}_i + \boldsymbol{\xi}(t), \quad (24)$$

where \mathbf{e}_i is an N -dimensional unit vector $\mathbf{e}_i := (0, \dots, \overset{(i)}{1}, \dots, 0)$, and the external force $\mathbf{f}_{\text{ex}}(t)$ is a three-dimensional vector.

A formal solution of Eq. (24) is given by

$$\mathbf{r}(t) = \frac{1}{\gamma} \int_0^t e^{-\frac{L}{\gamma}(t-\tau)} \cdot [\mathbf{f}_{\text{ex}}(\tau) \mathbf{e}_i + \boldsymbol{\xi}(\tau)] d\tau + e^{-\frac{L}{\gamma}t} \cdot \mathbf{r}(0). \quad (25)$$

Taking a contraction of this equation with \mathbf{e}_i and differentiating the result in terms of t , we have a GLE with the mobility-kernel representation as

$$\gamma \frac{d\mathbf{r}_i(t)}{dt} = \mathbf{f}_{\text{ex}}(t) + \int_0^t \psi(t-\tau) \mathbf{f}_{\text{ex}}(\tau) d\tau + \boldsymbol{\xi}_i + \boldsymbol{\xi}_i^m, \quad (26)$$

where $\psi(t)$ is a mobility kernel and $\boldsymbol{\xi}_i^m(t)$ is a correlated noise. They are defined by

$$\gamma\psi(t) := -\mathbf{e}_i \cdot L e^{-\frac{L}{\gamma}t} \cdot \mathbf{e}_i, \quad (27)$$

$$\boldsymbol{\xi}_i^m(t) := -\mathbf{e}_i \cdot L \left[\frac{1}{\gamma} \int_0^t e^{-\frac{L}{\gamma}(t-\tau)} \cdot \boldsymbol{\xi}(\tau) d\tau + e^{-\frac{L}{\gamma}t} \cdot \delta\mathbf{r}(0) \right] \quad (28)$$

where we set $\delta \mathbf{r}(0) := \mathbf{r}(0) - \mathbf{r}_i(0)\mathbf{1}_N$ and use $L \cdot \mathbf{1}_N = 0$ [Eq. (5)] in obtaining the last term in Eq. (28). The equation (26) was derived for the linear polymer models such as the Rouse model in Refs. [25, 26] by using normal mode techniques, but here we derive it without using normal modes for more general systems, i.e., the linear elastic network.

The resemblance of Eqs. (26)–(28) with Eqs. (17)–(19) is remarkable. For example, the vector $\mathbf{1}$ and matrix L' in Eq. (18) correspond to \mathbf{e}_i and L in Eq. (27). Moreover, as in the case of the resistance-kernel representation [Eq. (17)], there are a white noise $\xi_i(t)$ and a correlated noise $\xi_i^m(t)$ in Eq. (26). However, in this case, the two noise terms are not mutually independent, simply because $\xi_i^m(t)$ in Eq. (28) contains $\xi_i(t)$.

To confirm the FDR, we need to derive the covariant matrix $\langle \delta \mathbf{r}(0) \delta \mathbf{r}(0) \rangle$. Moreover, let us recall the assumption that the beads are in equilibrium at $t = 0$, at which the external force $\mathbf{f}_{\text{ex}}(t)$ is switched on. Under these assumptions, $\langle \delta \mathbf{r}'(0) \delta \mathbf{r}'(0) \rangle$ is again given by Eq. (22). Therefore, we obtain

$$\langle \delta \mathbf{r}(0) \delta \mathbf{r}(0) \rangle = k_B T M I_3, \quad (29)$$

where M is an $N \times N$ matrix; M is obtained by inserting zero vectors into the i th row and column of L'^{-1} . This matrix M is represented by a block matrix representation with a non-singular matrix J as

$$J M J^t = \begin{bmatrix} L'^{-1} & \mathbf{0} \\ \mathbf{0}^t & 0 \end{bmatrix}, \quad (30)$$

where J^t is the transposed matrix of J , and $\mathbf{0}$ and $\mathbf{0}^t$ is a column vector and a row vector, respectively. The matrix J (J^t) moves the i th row (column) of a matrix to the N th row (column), and j th row (column) with $i + 1 \leq j \leq N$ to $(j-1)$ th row (column), if it is multiplied to that matrix from the left (right). Note also that $A J^t J B = A B$ for any $N \times N$ matrices A and B [See Appendix B].

Although L does not have inversion, M plays the role of inversion as follows [12]:

$$\begin{aligned} (J L J^t)(J M J^t)(J L J^t) &= \begin{bmatrix} L' & l'_i \\ l_i^t & l'_i \cdot L'^{-1} \cdot l'_i \end{bmatrix} \\ &= \begin{bmatrix} L' & l'_i \\ l_i^t & l_{ii} \end{bmatrix} = J L J^t, \end{aligned} \quad (31)$$

where we use $l'_i = -L' \cdot \mathbf{1}$ [Eq. (9)] in the second equality. It follows that

$$L M L = L. \quad (32)$$

By using Eqs. (28) and (32), it is easy to show the FDR of the second kind

$$\begin{aligned} &\langle [\xi_i(t_1) + \xi_i^m(t_1)][\xi_i(t_2) + \xi_i^m(t_2)] \rangle \\ &= \gamma k_B T I_3 [2\delta(t_1 - t_2) + \psi(t_1 - t_2)]. \end{aligned} \quad (33)$$

Note that, if $t_1 < t_2$, we have $\langle \xi_i^m(t_1) \xi_i(t_2) \rangle = 0$, whereas $\langle \xi_i(t_1) \xi_i^m(t_2) \rangle = 2\gamma k_B T I_3 \psi(t_1 - t_2)$ due to the mutual dependence of the two noise terms.

If the external force $\mathbf{f}_{\text{ex}}(t)$ is absent, the left-hand side of Eq. (33) is equivalent to the velocity autocorrelation $\gamma^2 \langle \mathbf{v}_i(t_1) \mathbf{v}_i(t_2) \rangle$ [See Eq. (26)], where $\mathbf{v}_i(t)$ is the velocity of the i th bead defined by $\mathbf{v}_i = d\mathbf{r}_i/dt$. Thus, in the absence of $\mathbf{f}_{\text{ex}}(t)$, $\psi(t)$ is a velocity autocorrelation function at long time apart from a constant factor as

$$\langle \mathbf{v}_i(t) \mathbf{v}_i(0) \rangle = \frac{k_B T I_3}{\gamma} [2\delta(t) + \psi(t)]. \quad (34)$$

Therefore the negative sign in the right-hand side of Eq. (27) indicates that the velocity autocorrelation is antipersistent at $t > 0$, because L is positive semidefinite. A formula for the mean square displacement (MSD) can be readily obtained from Eq. (34).

C. Interrelation of two representations

Here, it is shown that the GLE with the resistance kernel [Eq. (35) below] can be transformed into the GLE with the mobility kernel [Eq. (26)] by using Laplace transforms. If there is a time-dependent external force $\mathbf{f}_{\text{ex}}(t)$ exerted on the tagged bead \mathbf{r}_i , the GLE with the resistance kernel in Eq. (17) is given by

$$\gamma \frac{d\mathbf{r}_i(t)}{dt} + \gamma \int_0^t \mu(t-\tau) \dot{\mathbf{r}}_i(\tau) d\tau = \mathbf{f}_{\text{ex}}(t) + \xi_i + \xi_i^r. \quad (35)$$

The Laplace transform of a function $\phi(t)$ is defined and denoted by $\hat{\phi}(s) := \int_0^\infty e^{-ts} \phi(t) dt$. Then, by the Laplace transform of Eq. (35), we have

$$\gamma \hat{\mathbf{v}}_i(s) = \frac{\hat{\mathbf{f}}_{\text{ex}}(s)}{1 + \hat{\mu}(s)} + \frac{\hat{\xi}_i(s) + \hat{\xi}_i^r(s)}{1 + \hat{\mu}(s)}. \quad (36)$$

To confirm the FDR for Eq. (36), a double Laplace transform is defined by

$$\langle \hat{\xi}_i(s_1) \hat{\xi}_i(s_2) \rangle := \int_0^\infty dt_1 \int_0^\infty dt_2 e^{-t_1 s_1} e^{-t_2 s_2} \langle \xi_i(t_1) \xi_i(t_2) \rangle. \quad (37)$$

Inserting Eq. (2) into Eq. (37), we have $\langle \hat{\xi}_i(s_1) \hat{\xi}_i(s_2) \rangle = 2\gamma k_B T I_3 / (s_1 + s_2)$. Similarly, the double Laplace transform of Eq. (23) is given by $\langle \hat{\xi}_i^r(s_1) \hat{\xi}_i^r(s_2) \rangle = \gamma k_B T I_3 [\hat{\mu}(s_1) + \hat{\mu}(s_2)] / (s_1 + s_2)$ [33]. From these relations, we obtain the FDR for Eq. (36) in the Laplace domain

$$\begin{aligned} &\left\langle \frac{\hat{\xi}_i(s_1) + \hat{\xi}_i^r(s_1)}{1 + \hat{\mu}(s_1)} \frac{\hat{\xi}_i(s_2) + \hat{\xi}_i^r(s_2)}{1 + \hat{\mu}(s_2)} \right\rangle \\ &= \gamma k_B T I_3 \frac{\frac{1}{1 + \hat{\mu}(s_1)} + \frac{1}{1 + \hat{\mu}(s_2)}}{s_1 + s_2}. \end{aligned} \quad (38)$$

where we used the fact that ξ_i and ξ_i^r are mutually independent.

Thus, the Laplace inversion of Eq. (36) yields a GLE with the mobility-kernel, which satisfies the FDR. Considering that the mobility kernel is the velocity autocorrelation function, it should be unique. Consequently, we conclude that Eq. (36) is equivalent to the Laplace transform of Eq. (26)

$$\gamma \hat{v}_i(s) = [1 + \hat{\psi}(s)] \hat{f}_{\text{ex}}(s) + \hat{\xi}_i(s) + \hat{\xi}_i^{\text{m}}(s). \quad (39)$$

Comparing Eqs. (36) and (39), we have a relation between the resistance and the mobility kernels

$$1 + \hat{\psi}(s) = \frac{1}{1 + \hat{\mu}(s)}, \quad (40)$$

and a relation between the corresponding correlated noises

$$\hat{\xi}_i^{\text{m}}(s) = \hat{\psi}(s) \hat{\xi}_i(s) + [1 + \hat{\psi}(s)] \hat{\xi}_i^{\text{r}}(s). \quad (41)$$

In Sec. IV D, in addition to the indirect proof given here, Eq. (40) is directly derived using normal modes.

D. Relation with projection operator formalism

Here, we derive another GLE using the projection operator method. The time evolution operator of the Langevin equation is given by the Hermitian conjugate of the Smoluchowski operator $\mathcal{L}_S^\dagger := k_B T / \gamma (\nabla - \beta [\nabla \Phi]) \cdot \nabla$ [29, Eq. (6.38)], where Φ is the potential energy and $\beta = 1/k_B T$. Because the potential Φ is arbitrary, the projection operator method can be applied to systems with nonlinear interactions such as those involving excluded volume effects. It is also possible to incorporate the HI into the operator \mathcal{L}_S^\dagger ; however, it is not considered here.

The operator \mathcal{L}_S^\dagger for the linear elastic network without the HI in Eq. (3) is given by

$$\mathcal{L}_S^\dagger = \frac{k_B T}{\gamma} \nabla^2 - \frac{1}{\gamma} (L I_3) : \mathbf{r} \nabla, \quad (42)$$

where ∇ is the $3N$ -dimensional gradient operator with respect to \mathbf{r} , and the double contractions, indicated by ':', are taken over the $3N$ -element pairs including I_3 (i.e., \mathbf{r} should be regarded as a $3N$ -dimensional vector).

Furthermore, we assume that the elastic network is confined by a spherically symmetric potential $\mathcal{U}(\mathbf{r}) = \sum_{k=1}^N U(r_k)$ to ensure the existence of an equilibrium state, which is necessary to define an inner product below. In particular, we employ a square-well potential such that $U(r) = 0$ for $r < R$, and $U(r) = \infty$ for $r > R$ with sufficiently large R . As a result of the spherical symmetry, the equilibrium state is statistically isotropic.

Now, let us define a projection operator \mathcal{P} as [28, Eq. (9.1.1)]

$$\mathcal{P} \mathbf{A}(\mathbf{r}) := (\mathbf{r}_i, \mathbf{A}(\mathbf{r})) (\mathbf{r}_i, \mathbf{r}_i)^{-1} \mathbf{r}_i, \quad (43)$$

where $\mathbf{A}(\mathbf{r})$ is a three-dimensional vector function of the phase space coordinates \mathbf{r} , the inner product (\bullet, \bullet) is a 3×3 tensor defined by

$$(\mathbf{A}, \mathbf{B}) := \int \mathbf{A}^*(\mathbf{r}) \mathbf{B}(\mathbf{r}) P_{\text{eq}}(\mathbf{r}) d\mathbf{r}, \quad (44)$$

$(\mathbf{r}_i, \mathbf{r}_i)^{-1}$ is the inversion of $(\mathbf{r}_i, \mathbf{r}_i)$, and $P_{\text{eq}}(\mathbf{r})$ is an equilibrium distribution. In Eq. (44), \mathbf{A}^* is the complex conjugate of \mathbf{A} . Moreover, the projection to the orthogonal complementary space is denoted as \mathcal{Q} , which is defined by

$$\mathcal{Q} := \mathcal{I} - \mathcal{P}, \quad (45)$$

with \mathcal{I} being an identity operator.

Let us define a function $\mathbf{c}(t, \mathbf{r})$ as

$$\mathbf{c}(t, \mathbf{r}) := e^{\mathcal{L}_S^\dagger t} \mathbf{r}_i. \quad (46)$$

Note that $\mathbf{c}(t, \mathbf{r})$ is closely related to $\mathbf{r}_i(t)$, but they are not equivalent, because the latter is a random process while the former is not. Thus, we employ the different notation $\mathbf{c}(t, \mathbf{r})$ instead of $\mathbf{r}_i(t)$. Hereafter, we denote it as $\mathbf{c}(t)$ instead of $\mathbf{c}(t, \mathbf{r})$ for brevity. As is well known, $\mathbf{c}(\mathbf{r})$ follows a GLE [29, Eq. (6.167)]

$$\gamma \frac{\partial \mathbf{c}}{\partial t} = \gamma e^{\mathcal{L}_S^\dagger t} \mathcal{P} \mathcal{L}_S^\dagger \mathbf{r}_i + \gamma \int_0^t \mathbf{M}(t - \tau) \cdot \mathbf{c}(\tau) d\tau + \boldsymbol{\xi}^{\text{pr}}(\mathbf{r}, t), \quad (47)$$

where the memory kernel $\mathbf{M}(t)$ and the fluctuating force $\boldsymbol{\xi}^{\text{pr}}(\mathbf{r}, t)$ are defined by

$$\mathbf{M}(t) := \frac{1}{\gamma^2} (\boldsymbol{\xi}^{\text{pr}}(t), \boldsymbol{\xi}^{\text{pr}}(0)) (\mathbf{r}_i, \mathbf{r}_i)^{-1}, \quad (48)$$

$$\boldsymbol{\xi}^{\text{pr}}(t) := \gamma e^{\mathcal{Q} \mathcal{L}_S^\dagger t} \mathcal{Q} \mathcal{L}_S^\dagger \mathbf{r}_i. \quad (49)$$

These equations (48) and (49) represents the FDR for the GLE in Eq. (47).

It is readily checked that

$$\mathcal{L}_S^\dagger \mathbf{r}_j = -\frac{1}{\gamma} \mathbf{l}_j \cdot \mathbf{r}, \quad (50)$$

where the contraction on the right-hand side is taken over the N -element pairs (i.e., \mathbf{r} is considered as an N -dimensional supervector. In the following, the dot product should be treated in the same way). It follows that

$$\mathcal{P} \mathcal{L}_S^\dagger \mathbf{r}_j = -\frac{l_{ij}}{\gamma} \mathbf{r}_i, \quad (51)$$

where we used the fact that the system is isotropic, and therefore $(\mathbf{r}_k, \mathbf{r}_i) = 0$ if $k \neq i$. By setting $j = i$ in Eq. (51) and applying $e^{\mathcal{L}_S^\dagger t}$ from the left, we have

$$e^{\mathcal{L}_S^\dagger t} \mathcal{P} \mathcal{L}_S^\dagger \mathbf{r}_i = -\frac{\mathbf{1} \cdot \mathbf{L}' \cdot \mathbf{1}}{\gamma} \mathbf{c}(t) = -\mu(0) \mathbf{c}(t) \quad (52)$$

where we used Eqs. (9) and (18). The equation (52) is an explicit expression of the first term on the right-hand side of Eq. (47).

By using Eqs. (45) and (51), we also have a projection on the orthogonal complementary space as

$$\mathcal{Q}\mathcal{L}_S^\dagger \mathbf{r}_j = \mathcal{L}_S^\dagger \mathbf{r}_j - \mathcal{P}\mathcal{L}_S^\dagger \mathbf{r}_j = -\frac{1}{\gamma} \mathbf{l}_j' \cdot \mathbf{r}'. \quad (53)$$

In particular, for $j = i$, the Eq. (53) is rewritten as

$$\mathcal{Q}\mathcal{L}_S^\dagger \mathbf{r}_i = \frac{1}{\gamma} \mathbf{1} \cdot L' \cdot \mathbf{r}', \quad (54)$$

where Eq. (9) is used. Moreover, combining Eq. (53) for all $j \neq i$, we obtain an important expression

$$\mathcal{Q}\mathcal{L}_S^\dagger \mathbf{r}' = -\frac{1}{\gamma} L' \cdot \mathbf{r}'. \quad (55)$$

These relations (54) and (55) clearly show that L' is closely related to $\mathcal{Q}\mathcal{L}_S^\dagger$, which is a time-evolution operator in the orthogonal complementary space.

By using Eqs. (53) and (55), we obtain an explicit expression for the fluctuating force as

$$\boldsymbol{\xi}^{\text{pr}}(t) = \mathbf{1} \cdot L' e^{-\frac{L'}{\gamma} t} \cdot \mathbf{r}'. \quad (56)$$

Unexpectedly, Eq.(56) is not equivalent to the non-thermal part of Eq. (19); this inconsistency shall be resolved shortly. Then, inserting Eq. (56) into the definition of $\mathbf{M}(t)$ in Eq. (48), and using a relation $(\mathbf{r}', \mathbf{r}') = (\mathbf{r}_i, \mathbf{r}_i) I_{N-1}$ due to the isotropy, the memory kernel $\mathbf{M}(t)$ is given by

$$\mathbf{M}(t) = -\frac{d\mu(t)}{dt} I_3, \quad (57)$$

where $\mu(t)$ is the resistance kernel given by Eq. (18).

Inserting Eqs. (52), (56) and (57) into Eq. (47), and then performing integration by parts, we have an equation for $\mathbf{c}(t)$ explicitly as

$$\gamma \frac{\partial \mathbf{c}(t)}{\partial t} + \gamma \int_0^t \mu(t-\tau) \dot{\mathbf{c}}(\tau) d\tau = \boldsymbol{\xi}^{\text{pr}}(t) - \gamma \mu(t) \mathbf{c}(0). \quad (58)$$

By using Eqs. (18) and (56), the right-hand side of Eq. (58) is rewritten as

$$\mathbf{1} \cdot L' e^{-\frac{L'}{\gamma} t} \cdot [\mathbf{r}' - \mathbf{c}(0) \mathbf{1}], \quad (59)$$

which is equivalent to the non-thermal part of Eq. (19), because $\mathbf{c}(0) = \mathbf{r}_i$. Thus, although Eq. (58) is similar to the GLE with the resistance kernel in Eq. (17), the thermal noise terms $\boldsymbol{\xi}_i$ and $\boldsymbol{\xi}'$ are absent as expected. Moreover, the term with $\mathbf{c}(0) \mathbf{1}$ in Eq. (59) is not a vector in the orthogonal complementary space, and thus it is not included in the fluctuating force $\boldsymbol{\xi}^{\text{pr}}$ in the projection operator scheme. In contrast, the corresponding term $\mathbf{r}_i(0) \mathbf{1}$ in Eq. (17) is included in the noise term $\boldsymbol{\xi}_i^{\text{r}}$ [Eq. (19)].

To obtain an example of an evolution equation, let us multiply \mathbf{r}_i/γ with Eq. (58) and take an ensemble average in terms of $P_{\text{eq}}(\mathbf{r})$, thereby obtaining [29, Eq. (6.150)]

$$\begin{aligned} \frac{d \langle \mathbf{r}_i(t) \mathbf{r}_i(0) \rangle}{dt} + \int_0^t \mu(t-\tau) \langle \dot{\mathbf{r}}_i(\tau) \mathbf{r}_i(0) \rangle d\tau \\ = -\mu(t) \langle \mathbf{r}_i(0) \mathbf{r}_i(0) \rangle. \end{aligned} \quad (60)$$

The same equation can be readily derived from Eq. (17).

IV. NORMAL MODES

To derive explicit expressions of the GLEs, it is necessary to utilize the normal modes. Diagonalization of L is straightforward [12] (See Sec. IV C), whereas that of L' is somewhat intricate to ensure translational symmetry in normal-mode equations. In addition, Eq. (40) is directly proved by using the normal modes.

A. Diagonalization of L'

Because L' is symmetric and positive definite (See Appendix A), there exist positive eigenvalues $\lambda_1, \dots, \lambda_{N-1}$ and corresponding eigenvectors $\mathbf{v}_1, \dots, \mathbf{v}_{N-1}$. That is, $L' \cdot [\mathbf{v}_1, \dots, \mathbf{v}_{N-1}] = [\lambda_1 \mathbf{v}_1, \dots, \lambda_{N-1} \mathbf{v}_{N-1}]$. Alternatively, this relation can be expressed as

$$L' Q = Q \Lambda, \quad (61)$$

where an $(N-1) \times (N-1)$ non-singular matrix Q is defined by

$$Q := [\mathbf{v}_1, \dots, \mathbf{v}_{N-1}], \quad (62)$$

and a diagonal matrix Λ is defined by $(\Lambda)_{jk} = \lambda_j \delta_{jk}$.

Moreover, we define constants $c_k > 0$ as $c_k := \mathbf{v}_k^2$, i.e., \mathbf{v}_k is not necessarily a unit vector as typically assumed. Instead, we impose a condition

$$\mathbf{1} \cdot Q = \mathbf{1}. \quad (63)$$

This condition implies that the sum of the elements of \mathbf{v}_k equals unity, thereby specifying the eigenvectors \mathbf{v}_k and the values of the constants c_k . Thanks to the condition in Eq. (63), normal-mode equations of motion remain translationally symmetric [See Eqs. (69) and (70)].

If the sum of the elements of \mathbf{v}_k vanishes, we consider c_k as ∞ . This is justified as follows. Such a mode k does not contribute to the dynamics of the tagged bead \mathbf{r}_i , due to $\mathbf{1} \cdot \mathbf{v}_k = 0$ and Eq. (18) with the spectral decomposition $L' = \sum_j \lambda_j \mathbf{v}_j \mathbf{v}_j$. We can remove the contribution from the mode k by formally setting $c_k = \infty$ in Eq. (73) below. This situation arises when the k th mode is independent of the tagged bead \mathbf{r}_i . An example of this is the ring polymer investigated in Sec. V B.

Left multiplication of Eq. (61) by Q^t results in the diagonalization of L' as

$$Q^t L' Q = C \Lambda \quad (64)$$

where Q^t is the transposed matrix of Q and a diagonal matrix C is defined as $(C)_{jk} = c_j \delta_{jk}$. Because $Q^t Q = C$ and C is non-singular, we have

$$Q^t Q C^{-1} = I_{N-1}, \quad (65)$$

$$Q C^{-1} Q^t = I_{N-1}. \quad (66)$$

Moreover, by using Eqs. (64)–(66), we have

$$L' = Q C^{-1} \Lambda Q^t. \quad (67)$$

This equation is rewritten as $Q^{-1} L' (Q^t)^{-1} = C^{-1} \Lambda$, and therefore we obtain

$$Q^t L'^{-1} Q = C \Lambda^{-1}. \quad (68)$$

B. Normal-mode GLE with resistance kernel

Multiplying $C^{-1} Q^t$ from the left of Eq. (14), inserting the identity $Q C^{-1} Q^t$ [Eq. (66)] behind L' , and using Eqs. (63) and (64), we have

$$\gamma C^{-1} \cdot \frac{d\mathbf{y}(t)}{dt} = -C^{-1} \Lambda \cdot [\mathbf{y}(t) - \mathbf{r}_i(t) \mathbf{1}] + \boldsymbol{\eta}(t), \quad (69)$$

where we define \mathbf{y} and $\boldsymbol{\eta}$ respectively as $\mathbf{y} := Q^t \cdot \mathbf{r}'$ and $\boldsymbol{\eta} := C^{-1} Q^t \cdot \boldsymbol{\xi}'$. Similarly, inserting Eq. (66) on both sides of L' in Eq. (15) and using Eqs. (63) and (64), we have

$$\gamma \frac{d\mathbf{r}_i(t)}{dt} = \mathbf{1} \cdot C^{-1} \Lambda \cdot [\mathbf{y}(t) - \mathbf{r}_i(t) \mathbf{1}] + \boldsymbol{\xi}_i(t). \quad (70)$$

Equations (69) and (70) form the normal-mode equations of motion.

Importantly, the noise $\boldsymbol{\eta}(t)$ in Eq. (69) satisfies the FDR in the form

$$\langle \boldsymbol{\eta}(t_1) \boldsymbol{\eta}(t_2) \rangle = 2\gamma C^{-1} k_B T I_3 \delta(t_1 - t_2), \quad (71)$$

which follows from Eq. (20). By multiplying Q^t and Q to Eq. (22) respectively from the left and the right, and using Eq. (68), we obtain a covariant matrix

$$\langle \delta\mathbf{y}(0) \delta\mathbf{y}(0) \rangle = k_B T C \Lambda^{-1} I_3. \quad (72)$$

where we define $\delta\mathbf{y}(0) := \mathbf{y}(0) - \mathbf{r}_i(0) \mathbf{1}$.

As in Sec. III A, it is possible to derive a normal-mode GLE by formally solving Eq. (69) and inserting the result into Eq. (70). But, it is straightforward to simply rewrite Eqs. (18) and (19) with the diagonal matrices Λ and C . By using Eqs. (67) and (63) in Eq. (18), the memory kernel $\mu(t)$ is rewritten as

$$\gamma \mu(t) = \text{tr} \left(C^{-1} \Lambda e^{-\frac{\Lambda}{\gamma} t} \right) = \sum_{j=1}^{N-1} \frac{\lambda_j}{c_j} e^{-\frac{\lambda_j}{\gamma} t}, \quad (73)$$

where tr denotes the trace of a matrix. Similarly, the correlated noise $\boldsymbol{\xi}_i^r(t)$ in Eq. (19) is rewritten as

$$\boldsymbol{\xi}_i^r(t) = \mathbf{1} \cdot C^{-1} \Lambda \left[\frac{C}{\gamma} \int_0^t e^{-\frac{\Lambda}{\gamma}(t-\tau)} \cdot \boldsymbol{\eta}(\tau) d\tau + e^{-\frac{\Lambda}{\gamma} t} \cdot \delta\mathbf{y}(0) \right]. \quad (74)$$

In addition, the FDR [Eq. (20)] for these normal-mode representations [Eqs. (73) and (74)] can be confirmed by using Eqs. (71) and (72).

Thus, we have the normal-mode GLE with the resistance kernel: Eq. (17) along with Eqs. (73) and (74). Since we have derived the GLE without utilizing the normal mode in the previous section, the diagonalization process becomes a straightforward problem in linear algebra. Note also that the matrix C appears in these equations instead of Q ; this should be an advantage of the diagonalization procedure presented in this subsection.

C. Normal-mode GLE with mobility kernel

Because L is symmetric, it can be diagonalized with an orthogonal matrix P as $P^t L P = \Sigma$, where Σ is a diagonal matrix defined by using eigenvalues σ_j as $(\Sigma)_{jk} = \sigma_j \delta_{jk}$. We set that $\sigma_1 = 0$ and $\sigma_j > 0$ ($j \geq 2$). Multiplying P^t to Eq. (24) from the left, we have

$$\gamma \frac{d\mathbf{z}(t)}{dt} = -\Sigma \cdot \mathbf{z}(t) + \mathbf{f}_{\text{ex}}(t) P^t \cdot \mathbf{e}_i + \boldsymbol{\zeta}(t), \quad (75)$$

where we define \mathbf{z} and $\boldsymbol{\zeta}$ as $\mathbf{z} := P^t \cdot \mathbf{r}$ and $\boldsymbol{\zeta} := P^t \cdot \boldsymbol{\xi}$. The first mode $\mathbf{z}_1(t)$, which corresponds to the zero eigenvalue $\sigma_1 = 0$ with the associated eigenvector $\mathbf{1}_N / \sqrt{N}$, describes the center-of-mass motion.

Moreover, $\boldsymbol{\zeta}(t)$ in Eq. (75) satisfies the FDR

$$\langle \boldsymbol{\zeta}(t) \boldsymbol{\zeta}(t') \rangle = 2\gamma k_B T \delta(t - t') I_3 I_N, \quad (76)$$

which follows from Eq. (4) and the orthogonality $P^t P = I_N$. By multiplying P^t and P to Eq. (29) respectively from the left and the right, and using Eq. (68), we obtain a covariant matrix

$$\langle \delta\mathbf{z}(0) \delta\mathbf{z}(0) \rangle = k_B T P^t M P I_3, \quad (77)$$

where $\delta\mathbf{z}(0)$ is defined by $\delta\mathbf{z}(0) := \mathbf{z}(0) - \mathbf{r}_i(0) P^t \cdot \mathbf{1}_N$.

It is possible to derive a normal-mode GLE with the mobility kernel by applying $\mathbf{e}_i \cdot P$ to a formal solution of Eq. (75) and then differentiating the resulting equation in terms of t . However, here the GLE is obtained by simply replacing L in Eqs. (27) and (28) with $P \Sigma P^t$. Thus, we have

$$\gamma \psi(t) = -\mathbf{e}_i \cdot P \Sigma e^{-\frac{\Sigma}{\gamma} t} P^t \cdot \mathbf{e}_i = -\sum_{j=1}^N p_{ij}^2 \sigma_j e^{-\frac{\sigma_j}{\gamma} t}, \quad (78)$$

$$\boldsymbol{\xi}_i^m(t) = -\mathbf{e}_i \cdot P \Sigma \left[\frac{1}{\gamma} \int_0^t e^{-\frac{\Sigma}{\gamma}(t-\tau)} \cdot \boldsymbol{\zeta}(\tau) d\tau + e^{-\frac{\Sigma}{\gamma} t} \cdot \delta\mathbf{z}(0) \right], \quad (79)$$

where p_{ij} is the (i, j) entry of the matrix P . In addition, the FDR [Eq. (33)] for these normal-mode representations [Eqs. (78) and (79)] can be confirmed by using Eqs. (76) and (77). Thus, we have the normal-mode GLE with the mobility kernel: Eq. (26) along with Eqs. (78) and (79).

D. Direct proof of Eq. (40)

The two memory kernels in Eqs. (73) and (78) are interrelated through Eq. (40). However, the relation is not immediately obvious even from these normal-mode expressions [Eqs. (73) and (78)]. Here, we directly prove Eq. (40) by utilizing a formula concerning Schur complements.

First, Laplace transform of Eq. (73) is given by

$$1 + \hat{\mu}(s) = 1 + \sum_{j=1}^N \frac{\lambda_j}{c_j} \frac{1}{\tilde{s} + \lambda_j}, \quad (80)$$

where we set $\tilde{s} := \gamma s$. Similarly, Laplace transform of Eq. (78) is given by

$$1 + \hat{\psi}(s) = 1 - \sum_{j=1}^N p_{ij}^2 \frac{\sigma_j}{\tilde{s} + \sigma_j} = \sum_{j=1}^N p_{ij}^2 \frac{\tilde{s}}{\tilde{s} + \sigma_j}, \quad (81)$$

where $\sum_{j=1}^N p_{ij}^2 = 1$ is used. We show that the left-hand sides of Eqs. (80) and (81) are in the reciprocal relation indicated in Eq. (40).

Let us set $A := -L - \tilde{s}I_N$ and $A' := -L' - \tilde{s}I_{N-1}$. Using a formula for the determinant of the Schur complement [34, Sec. 0.8.5.1], we have

$$\begin{aligned} \det A &= \det A' (-l_{ii} - \tilde{s} - \mathbf{l}'_i \cdot A'^{-1} \cdot \mathbf{l}'_i) \\ &= \det A' (-l_{ii} - \tilde{s} - \mathbf{1} \cdot L' A'^{-1} L' \cdot \mathbf{1}), \end{aligned} \quad (82)$$

where Eq. (9) is used. Here, A'^{-1} is the resolvent of $-L'$ and is calculated by $A'^{-1} = -\int_0^\infty e^{-\tilde{s}t} e^{-L't} dt$ [29]. Consequently, we have a diagonalized expression of $L' A'^{-1} L'$ as follows:

$$\begin{aligned} \mathbf{1} \cdot L' A'^{-1} L' \cdot \mathbf{1} &= \mathbf{1} \cdot C^{-1} \Lambda^2 (-\Lambda - \tilde{s}I_{N-1})^{-1} \cdot \mathbf{1} \\ &= - \sum_{j=1}^{N-1} \frac{\lambda_j^2}{c_j} \frac{1}{\lambda_j + \tilde{s}}, \end{aligned} \quad (83)$$

where Eq. (67) is utilized.

Moreover, From Eqs. (5) and (9), we have $l_{ii} = \mathbf{1} \cdot L' \cdot \mathbf{1}$. Consequently, by applying the vector $\mathbf{1}$ from both sides of Eq. (67), we have

$$l_{ii} = \mathbf{1} \cdot L' \cdot \mathbf{1} = \sum_{j=1}^{N-1} \frac{\lambda_j}{c_j}. \quad (84)$$

Inserting Eqs. (83) and (84) into Eq. (82), we have

$$\frac{1}{1 + \hat{\mu}(s)} = -\tilde{s} \frac{\det A'}{\det A} = -\tilde{s} (A^{-1})_{ii}, \quad (85)$$

where $(A^{-1})_{ii}$ is the (i, i) entry of A^{-1} , and a formula of the inverse matrix is used in the second equality.

Similarly, A^{-1} , which is the resolvent of $-L$, can be calculated as

$$A^{-1} = P(-\Sigma - \tilde{s}I_N)^{-1} P^t. \quad (86)$$

It follows that

$$-\tilde{s} (A^{-1})_{ii} = \sum_{j=1}^N p_{ij}^2 \frac{\tilde{s}}{\tilde{s} + \sigma_j} = 1 + \hat{\psi}(s), \quad (87)$$

where Eq. (81) is used. From Eqs. (85) and (87), we obtain Eq. (40), thereby completing the proof.

E. Asymptotics

Here, we briefly discuss short-time and long-time diffusion of the tagged bead. For small and large \tilde{s} , Eq. (81) is approximately expressed as

$$1 + \hat{\psi}(s) \simeq \begin{cases} 1 & (\tilde{s} \gg \sigma_N), \\ p_{i1}^2 = \frac{1}{N} & (\tilde{s} \ll \sigma_2), \end{cases} \quad (88)$$

where we used $\sigma_1 = 0$, and $p_{i1} = 1/\sqrt{N}$. σ_2 and σ_N are the smallest and largest positive eigenvalues of L , respectively. Laplace inversion of Eq. (88) yields the velocity autocorrelation [Eq. (34)] as

$$\langle \mathbf{v}_i(t) \mathbf{v}_i(0) \rangle \simeq \begin{cases} \frac{2k_B T}{\gamma} \delta(t) I_3 & (t \ll \gamma/\sigma_N), \\ \frac{2k_B T}{\gamma N} \delta(t) I_3 & (t \gg \gamma/\sigma_2). \end{cases} \quad (89)$$

The short-time and long-time diffusion coefficient can be obtained using the Green-Kubo formula [35]:

$$D = \frac{1}{3} \int_0^\infty \langle \mathbf{v}_i(t) \cdot \mathbf{v}_i(0) \rangle = \begin{cases} \frac{k_B T}{\gamma} & (t \ll \gamma/\sigma_N), \\ \frac{k_B T}{\gamma N} & (t \gg \gamma/\sigma_2). \end{cases} \quad (90)$$

The long-time diffusivity $k_B T/\gamma N$ is the diffusion coefficient for the center of mass motion. Behaviors at intermediate timescales depend on the details of the system.

V. SIMPLE POLYMER MODELS

In this section, we investigate the Rouse model [7, 8] and the ring polymer as simple examples of the linear elastic network. In particular, for the Rouse model, the memory kernels and the correlated noises depend on the position of the tagged bead, resulting in different GLEs for the end bead and the middle bead.

A. Rouse model

1. Resistance kernel

First, let us begin with a derivation of the resistance kernel $\mu(t)$. The interaction matrix L in Eq. (3) for the Rouse model is given by

$$L = \kappa \begin{pmatrix} 1 & -1 & 0 & 0 & & \\ -1 & 2 & -1 & 0 & & \\ 0 & -1 & 2 & -1 & & \\ & & & \ddots & & \\ & & & & -1 & 2 & -1 \\ & & & & 0 & -1 & 1 \end{pmatrix}, \quad (91)$$

where κ is the spring constant. The matrix L' is then obtained by removing the i th row and column from L as

$$L' = \kappa \begin{pmatrix} L_1 & 0 \\ 0 & L_2 \end{pmatrix}, \quad (92)$$

where L_1 is an $(i-1) \times (i-1)$ matrix and L_2 is an $(N-i) \times (N-i)$ matrix. They are defined respectively by

$$L_1 = \kappa \begin{pmatrix} 1 & -1 & 0 & & \\ -1 & 2 & -1 & & \\ & & \ddots & & \\ & & & -1 & 2 & -1 \\ & & & 0 & -1 & 2 \end{pmatrix}. \quad (93)$$

and

$$L_2 = \kappa \begin{pmatrix} 2 & -1 & 0 & & \\ -1 & 2 & -1 & & \\ & & \ddots & & \\ & & & -1 & 2 & -1 \\ & & & 0 & -1 & 1 \end{pmatrix}. \quad (94)$$

The eigenvalues and eigenvectors of L_1 and L_2 can be obtained by solving recursion relations (See Ref. [36, Sec.XVI.3] for a procedure). The eigenvalues of L_1 is given by [24]

$$\lambda_k = 4\kappa \sin^2 \frac{\beta_k \pi}{2}, \quad (k = 1, \dots, i-1), \quad (95)$$

with $\beta_k := (2k-1)/(2i-1)$. The associated eigenvector \mathbf{v}_k of L_1 is given by

$$v_{kq} = b_k \cos \frac{\beta_k}{2} (2q-1)\pi, \quad (q = 1, \dots, i-1). \quad (96)$$

Here, b_k is a constant, which can be obtained with the condition in Eq. (63), or equivalently, $\sum_q v_{kq} = 1$. Thus, we have

$$b_k = (-1)^{k+1} 2 \tan \frac{\beta_k \pi}{2}. \quad (97)$$

Then, the diagonal elements of C , which are defined by $c_k = \mathbf{v}_k^2$ in Sec. III, can be determined as

$$c_k = \sum_{q=1}^{i-1} v_{kq}^2 = \frac{1}{2} \sum_{q=1}^{2i-1} v_{kq}^2 = (2i-1) \tan^2 \frac{\beta_k \pi}{2}, \quad (98)$$

where, in the second equality, we used $v_{ki} = 0$ and $v_{kq}^2 = v_{k(2i-q)}^2$ for $q = 1, \dots, i-1$. Replacing i with $i' := N-i+1$ and β_k with $\beta'_k := (2k-1)/(2i'-1)$ in Eqs. (95)–(98), we obtain similar results for L_2 .

Accordingly, the resistance kernel in Eq. (73) is given by

$$\gamma \mu(t) = \frac{4\kappa}{2i-1} \sum_{k=1}^{i-1} \cos^2 \frac{\beta_k \pi}{2} e^{-\frac{4\kappa t}{\gamma} \sin^2 \beta_k \pi / 2} + \frac{4\kappa}{2i'-1} \sum_{k=1}^{i'-1} \cos^2 \frac{\beta'_k \pi}{2} e^{-\frac{4\kappa t}{\gamma} \sin^2 \beta'_k \pi / 2}. \quad (99)$$

If the tagged bead is the middle one, i.e., $i = i'$, the Eq. (99) is consistent with a result presented in Ref. [24]. However, Eq. (99) is valid for arbitrary i ($1 \leq i \leq N$).

If $i, i' \gg 1$, modes with small $k \ll i, i'$ are dominant at long time $t \gg \gamma/\kappa$, and therefore approximations $\sin \beta_k \pi / 2 \approx \beta_k \pi / 2$ and $\cos \beta_k \pi / 2 \approx 1$ are justified [24]. Let us denote this time scale as $t_0 := \gamma/\kappa$. As a result, we obtain an expression of the memory kernel for the continuous Rouse model studied in Ref. [22]. In particular, an integral approximation reveals power-law decay [22, 24]

$$\mu(t) \approx 2 \left(\frac{1}{\pi t_0 t} \right)^{1/2}, \quad (100)$$

which is valid for $t_0 \ll t \ll t^*$ with t^* being the longest relaxation time; for example, if $i \sim i'$, then $t^* = t_0(2i-1)^2/\pi^2$, and $\mu(t)$ decays exponentially at $t \geq t^*$. Note that Eq. (100) is independent of i , whereas t^* depends on i . The equation (100) is consistent with a result for the middle bead (i.e., $i = i'$) reported in Ref. [24].

If $i \gg 1$ and $i' \sim 1$, however, we obtain a different result, because the second term in the right-hand side of Eq. (99) is negligible at $t \gg t_0$. It follows that

$$\mu(t) \approx \left(\frac{1}{\pi t_0 t} \right)^{1/2}. \quad (101)$$

Thus, the resistance kernel $\mu(t)$ depends on the location of the tagged bead i in the Rouse chain. The Laplace transforms of Eqs. (100) and (101) yield

$$1 + \hat{\mu}(s) \approx \begin{cases} 2(t_0 s)^{-1/2} & (i, i' \sim \frac{N}{2}), \\ (t_0 s)^{-1/2} & (i \sim 1 \text{ or } i' \sim 1). \end{cases} \quad (102)$$

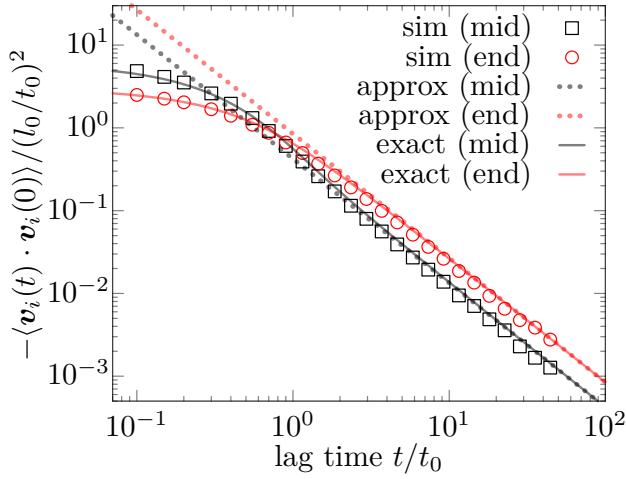


FIG. 2. Velocity autocorrelation function $\langle \mathbf{v}_i(t) \cdot \mathbf{v}_i(0) \rangle$ for a tagged bead in the Rouse chain is presented with units of $t_0 := \gamma/\kappa$ and $l_0 = (k_B T/\kappa)^{1/2}$ (See Appendix C). Because the velocity autocorrelation is negative, its absolute values are displayed in log-log form. In the simulation, the number of beads is set as $N = 101$. The tagged bead is the middle bead ($i = 51$; squares) and an end bead ($i = 1$; circles). The solid lines represent the exact theory from Eq. (105), while the dotted lines represent the approximate theory from Eq. (108).

2. Mobility kernel

Next, we derive the mobility kernel $\psi(t)$ for the Rouse model. The eigenvalues and eigenvectors of L in Eq. (91) are explicitly given by [37]

$$\sigma_k = 4\kappa \sin^2 \frac{k\pi}{2N}, \quad (103)$$

$$p_{qk} = \sqrt{\frac{2 - \delta_{k0}}{N}} \cos \frac{(2q-1)k\pi}{2N}, \quad (104)$$

with $k = 0, \dots, N-1$. Here, the eigenvectors are normalized as $\mathbf{p}_k^2 = 1$ [See Sec. IV C]. Inserting Eqs. (103) and (104) into Eq. (78), we obtain the mobility kernel for the Rouse model as

$$\psi(t) = -\frac{8\kappa}{N\gamma} \sum_{k=1}^{N-1} \cos^2 \frac{(2i-1)k\pi}{2N} \sin^2 \frac{k\pi}{2N} e^{-\frac{4\kappa t}{\gamma} \sin^2 \frac{k\pi}{2N}}. \quad (105)$$

If $t \gg t_0$, then modes with small k are dominant, and therefore the approximation $\sin \pi k/2N \approx \pi k/2N$ can be justified. Furthermore, if $i \sim N/2$, the mobility kernel in Eq. (105) is approximated as

$$\psi(t) \approx -\frac{\pi^2 \kappa}{N^3 \gamma} \sum_{k=1}^{N-1} k^2 e^{-\left(\frac{k\pi}{N}\right)^2 \frac{\kappa}{\gamma} t}, \quad (106)$$

where we used $\cos^2 \pi(2i-1)k/2N \approx 1/2$. In contrast, if $i \sim 1$, we obtain

$$\psi(t) \approx -\frac{2\pi^2 \kappa}{N^3 \gamma} \sum_{k=1}^{N-1} k^2 e^{-\left(\frac{k\pi}{N}\right)^2 \frac{\kappa}{\gamma} t}, \quad (107)$$

where we used $\cos \pi k/2N \approx 1$. This Equation (107) coincides with a result for the Rouse model reported in Ref. [25], if we set a parameter τ_0 employed in that paper as $\tau_0 = \gamma/\pi^2 \kappa$.

Integral approximations of Eqs. (106) and (107) reveal power-law decay:

$$\psi(t) \approx \begin{cases} -\frac{1}{4\sqrt{\pi t_0}} \left(\frac{t_0}{t}\right)^{3/2} & (i, i' \sim \frac{N}{2}), \\ -\frac{1}{2\sqrt{\pi t_0}} \left(\frac{t_0}{t}\right)^{3/2} & (i \sim 1 \text{ or } i' \sim 1). \end{cases} \quad (108)$$

The formulas in Eq. (108) are valid for $t_0 \ll t \ll t^*$, and correspond to the two formulas for the resistance kernel $\psi(t)$ in Eqs. (100) and (101). In fact, the Laplace transforms of Eq. (108) yield [38]

$$1 + \hat{\psi}(s) \approx \begin{cases} \frac{1}{2} (t_0 s)^{1/2} & (i, i' \sim \frac{N}{2}), \\ (t_0 s)^{1/2} & (i \sim 1 \text{ or } i' \sim 1), \end{cases} \quad (109)$$

where we used $\hat{\psi}(0) = -1$ from Eq. (27). By comparing Eq. (109) with Eq. (102), it is found that the relation in Eq. (40) still holds under these approximations.

The mobility kernel is equivalent to the velocity autocorrelation if the external force is absent [See Eq. (34)]. Therefore, from Eq. (108), it can be observed that the velocity autocorrelation for the end beads is stronger than that for the middle bead. This observation is consistent with the similar result for a polymerized membrane [39]. The velocity autocorrelation functions for tagged beads are numerically calculated and presented in Fig. 2. The exact formula in Eq. (105), displayed with solid lines in Fig. 2, is consistent with the numerical results across all time scales, while the long-time approximations in Eq. (108), displayed with dotted lines, are consistent with the numerical results at long times $t/t_0 > 1$.

Moreover, the power-law decay in the velocity autocorrelation $t^{-3/2}$ leads to subdiffusion, characterized by the MSD $\sim t^{1/2}$ for the intermediate time scale $t_0 \ll t \ll t^*$ [22]. At short and long times, normal diffusion is observed, as generally demonstrated in Eq. (90).

B. Ring polymer

1. Resistance kernel

The interaction matrix L in Eq. (3) for the ring polymer is given by

$$L = \kappa \begin{pmatrix} 2 & -1 & 0 & 0 & & 0 & -1 \\ -1 & 2 & -1 & 0 & & & \\ 0 & -1 & 2 & -1 & & & \\ & & & \ddots & & & \\ & & & & -1 & 2 & -1 \\ -1 & 0 & & & 0 & -1 & 2 \end{pmatrix}. \quad (110)$$

For the ring polymer, all the beads are identical, and therefore we define the matrix L' by removing the N th

row and column from L as

$$L' = \kappa \begin{pmatrix} 2 & -1 & 0 & & \\ -1 & 2 & -1 & & \\ & & \ddots & \ddots & \\ & & & -1 & 2 & -1 \\ & & & 0 & -1 & 2 \end{pmatrix}. \quad (111)$$

The eigenvalues and eigenvectors of L' can be obtained by solving recursion relations. The eigenvalues of L' is given by

$$\lambda_k = 4\kappa \sin^2 \frac{\pi k}{2N}, \quad (k = 1, \dots, N-1). \quad (112)$$

The associated eigenvector of L , \mathbf{v}_k , is given by

$$v_{kq} = b_k \sin \frac{\pi k q}{N}, \quad (q = 1, \dots, N-1). \quad (113)$$

Here, b_k is a constant, which can be obtained with the condition in Eq. (63), or equivalently, $\sum_q v_{kq} = 1$. Thus, we have

$$b_k = \begin{cases} \tan \frac{\pi k}{2N} & (k : \text{odd}), \\ \infty & (k : \text{even}), \end{cases} \quad (114)$$

where, for even k , we have $\sum_q v_{kq} = 0$, and therefore we formally set as $b_k = \infty$; this results in $c_k = \infty$ in Eq. (115) below (See also Sec. IV A for a general explanation). Then, the diagonal elements of C , which are defined by $c_k = \mathbf{v}_k^2$ in Sec. III, can be determined as

$$c_k = \sum_{q=1}^{N-1} v_{kq}^2 = \sum_{q=1}^N v_{kq}^2 = \begin{cases} \frac{N}{2} \tan^2 \frac{\pi k}{2N} & (k : \text{odd}), \\ \infty & (k : \text{even}). \end{cases} \quad (115)$$

Accordingly, the resistance kernel in Eq. (73) is given by

$$\gamma\mu(t) = \frac{8\kappa}{N} \sum_{k=1, \text{odd}}^{N-1} \cos^2 \frac{\pi k}{2N} e^{-\frac{4\kappa t}{\gamma} \sin^2 \frac{\pi k}{2N}}. \quad (116)$$

At long time $t \gg t_0 = \gamma/\kappa$, modes with small $k \ll N$ are dominant and therefore approximations $\sin \pi k/2N \approx \pi k/2N$ and $\cos \pi k/2N \approx 1$ are justified. An integral approximation reveals the same power-law decay as the middle bead in the Rouse model [Eq. (100)].

2. Mobility kernel

Here, we derive the mobility kernel $\psi(t)$ for the ring polymer. The eigenvalues and eigenvectors of the symmetric circulant matrix L in Eq. (110) are well known as [40]

$$\sigma_k = 4\kappa \sin^2 \frac{k\pi}{N}, \quad (117)$$

$$p_{qk} = \sqrt{\frac{2}{N}} \cos \left(\frac{2\pi k q}{N} + \frac{\pi}{4} \right), \quad (118)$$

for $k = 0, \dots, N-1$. Note that the eigenvalues are degenerate because $\sigma_k = \sigma_{N-k}$; hence, the term $\pi/4$ in the eigenvectors is necessary to ensure orthogonality. The eigenvectors are normalized as $\mathbf{p}_k^2 = 1$.

Inserting Eqs. (117) and (118) into Eq. (78), we obtain the mobility kernel for the ring polymer as

$$\psi(t) = -\frac{4\kappa}{N\gamma} \sum_{k=1}^{N-1} \sin^2 \frac{k\pi}{N} e^{-\frac{4\kappa t}{\gamma} \sin^2 \frac{k\pi}{N}}. \quad (119)$$

For $t \gg t_0$, modes with small $k \sim 1$ and large $k \sim N$ are dominant. Therefore, using the approximation $\sin \pi k/N \approx \pi k/N$, we should also double the formula. Thus, we obtain

$$\psi(t) \approx -\frac{8\pi^2 \kappa}{N^3 \gamma} \sum_{k=1}^{N-1} k^2 e^{-\left(\frac{2k\pi}{N}\right)^2 \frac{\kappa}{\gamma} t}. \quad (120)$$

An integral approximation of Eq. (120) reveals exactly the same power-law decay as the middle bead of the Rouse model [the first expression in Eq. (108)].

VI. HYDRODYNAMIC INTERACTION

In this section, the GLE with the mobility kernel is derived for the elastic network with the HI [Eq. (11)]; however, it is shown that the GLE with the resistance kernel cannot be derived using the method in Sec. III A. We consider Eq. (11) with the external force $\mathbf{f}_{\text{ex}}(t)$ applied to the tagged bead i :

$$\frac{d\mathbf{r}(t)}{dt} = -L_H \cdot \mathbf{r}(t) + \mathbf{h}_i \mathbf{f}_{\text{ex}}(t) + \boldsymbol{\xi}_H(t), \quad (121)$$

where $\mathbf{f}_{\text{ex}}(t)$ is a three-dimensional vector, and \mathbf{h}_i is the i th column vector of the mobility matrix H .

A. GLE with two kernels

Following the derivations of Eqs. (14) and (15) in Sec. III A, a generalization to the case with the HI can be obtained from Eq. (121) as

$$\frac{d\mathbf{r}'(t)}{dt} = -L'_H \cdot [\mathbf{r}'(t) - \mathbf{r}_i(t)\mathbf{1}] + \boldsymbol{\xi}'_H(t), \quad (122)$$

$$\frac{d\mathbf{r}_i(t)}{dt} = \bar{\mathbf{w}}' \cdot L'_H \cdot [\mathbf{r}'(t) - \mathbf{r}_i(t)\mathbf{1}] + \boldsymbol{\xi}_{Hi}(t), \quad (123)$$

where Eq. (13) is used, and we set $\bar{\mathbf{w}}' := \mathbf{w}/w_i$ and $\boldsymbol{\xi}_{Hi} := (\boldsymbol{\xi}_H)_i$. Note that the law of action and reaction is violated due to the HI in contrast to the case without HI [Eqs. (14) and (15)].

In exactly the same manner as the derivation of

Eq. (17), we obtain a GLE with mixed kernels,

$$\begin{aligned} \frac{d\mathbf{r}_i(t)}{dt} + \int_0^t \mu_H(t-\tau) \dot{\mathbf{r}}_i(\tau) d\tau \\ = \int_0^t \psi_H(t-\tau) \mathbf{f}_{\text{ex}}(\tau) d\tau + \boldsymbol{\xi}_{Hi}(t) + \boldsymbol{\xi}_{Hi}^{\text{mix}}(t). \end{aligned} \quad (124)$$

The resistance and mobility kernels in Eq. (124), $\mu_H(t)$ and $\psi_H(t)$, and the correlated noise $\boldsymbol{\xi}_{Hi}^{\text{mix}}(t)$ are defined by

$$\mu_H(t) := \bar{\mathbf{w}}' \cdot L'_H e^{-L'_H t} \cdot \mathbf{1}, \quad (125)$$

$$\psi_H(t) := \bar{\mathbf{w}}' \cdot L'_H e^{-L'_H t} \cdot \mathbf{h}'_i, \quad (126)$$

$$\boldsymbol{\xi}_{Hi}^{\text{mix}}(t) :=$$

$$\bar{\mathbf{w}}' \cdot L'_H \cdot \left[\int_0^t e^{-L'_H(t-\tau)} \cdot \boldsymbol{\xi}'_H(\tau) d\tau + e^{-L'_H t} \cdot \delta \mathbf{r}'(0) \right], \quad (127)$$

where $\bar{\mathbf{w}}' := \mathbf{w}'/w_i$, and \mathbf{h}'_i is the vector obtained by removing the i th entry of \mathbf{h}_i .

Thus, we arrived at a GLE with two kernels, and it is not possible to derive the GLE with only the resistance kernel using the method described in Sec. III A. This is because Eq. (121) is in a mobility representation. In other words, to obtain the GLE with the resistance kernel, one would need to start from a resistance representation; however, the method in Sec. III A is not applicable in that case.

An exception is the case in which the beads have different masses and the HI is absent. In this case, the mobility matrix H is diagonal, and therefore $\mathbf{h}'_i = \mathbf{0}$. Consequently, Eq. (124) reduces to the GLE with the resistance kernel, satisfying the FDR $\langle \boldsymbol{\xi}_{\text{all}}(t) \boldsymbol{\xi}_{\text{all}}(0) \rangle = k_B T h_{ii} I_3 [\mu_H(t) + 2\delta(t)]$, where h_{ii} is the (i, i) entry of H , and $\boldsymbol{\xi}_{\text{all}} := \boldsymbol{\xi}_{Hi} + \boldsymbol{\xi}_{Hi}^{\text{mix}}$.

B. GLE with mobility kernel

In contrast to the resistance representation in the previous subsection, the GLE with a mobility representation can be derived from Eq. (121) using the method described in Sec. III B as

$$\frac{d\mathbf{r}_i(t)}{dt} = h_{ii} \mathbf{f}_{\text{ex}}(t) + \int_0^t \psi_H(t-\tau) \mathbf{f}_{\text{ex}}(\tau) d\tau + \boldsymbol{\xi}_{Hi} + \boldsymbol{\xi}_{Hi}^{\text{m}}, \quad (128)$$

where the mobility kernel $\psi_H(t)$ and the correlated noise $\boldsymbol{\xi}_{Hi}^{\text{m}}(t)$ are defined as

$$\psi_H(t) := -\mathbf{e}_i \cdot L_H e^{-L_H t} \cdot \mathbf{h}_i, \quad (129)$$

$$\boldsymbol{\xi}_{Hi}^{\text{m}}(t) :=$$

$$-\mathbf{e}_i \cdot L_H \cdot \left[\int_0^t e^{-L_H(t-\tau)} \cdot \boldsymbol{\xi}_H(\tau) d\tau + e^{-L_H t} \cdot \delta \mathbf{r}(0) \right]. \quad (130)$$

Thus, the HI affects the relaxation property of the tagged bead. If we define $\boldsymbol{\xi}_{\text{all}} := \boldsymbol{\xi}_{Hi} + \boldsymbol{\xi}_{Hi}^{\text{m}}$, then the FDR is given by $\langle \boldsymbol{\xi}_{\text{all}}(t) \boldsymbol{\xi}_{\text{all}}(0) \rangle = k_B T I_3 [\psi_H(t) + 2h_{ii}\delta(t)]$.

VII. DISCUSSION

Previous studies have derived two types of the GLEs—one with the resistance kernel and the other with the mobility kernel—for linear polymer models by using normal modes [21–27]. In this paper, these GLEs are derived for a broader class of models: the linear elastic networks. Notably, our derivation does not rely on normal modes, and this makes the derivation process much clearer. We also show that the two GLEs are interconnected through Laplace transform.

These derivations have been made possible thanks to the supervector notation introduced in Sec. II B. This notation is so useful that it may be possible to derive a GLE for the case in which two beads are simultaneously tagged. To derive such a GLE, we should remove two rows and two columns from L (i th and j th rows and columns, say). It is anticipated that an interaction between tagged beads, mediated by the other beads, might yield an additional coupling. Such a theoretical study should be crucial for interpreting data from particle-tracking experiments, especially as recent advances in experimental techniques enable simultaneously tracking multiple points within a chromatin domain [18]. Furthermore, for understanding the fluctuations of distances between beads, such as the end-to-end distance [19, 27, 41], the GLE with two tagged beads would become a useful tool.

In general elastic networks, the equilibrium distance $d_{ij} := |\mathbf{r}_i - \mathbf{r}_j|$ between two beads at $T = 0$ is non-zero [1, 42]; contrastingly, in the simple elastic network discussed in this article, the distance d_{ij} is assumed to be zero. Thus, in general elastic networks, the matrix LI_3 should be replaced with a $3N \times 3N$ matrix \tilde{L} . As a result, in addition to the zero modes (eigenvectors with the zero eigenvalue) due to translational symmetry, \tilde{L} also has zero modes due to rotational symmetry. Therefore, the matrix \tilde{L}' , obtained by removing the tagged particle coordinates \mathbf{r}_i , is not positive definite and is singular. Consequently, the derivation of the GLE with the resistance kernel in Sec. III A must be modified; specifically, a pseudo-inverse similar to M in Eq. (32) should be employed.

If the external force is absent, the GLE with the mobility kernel in Eq. (26) becomes a simple Langevin equation with a correlated noise

$$\gamma \dot{\mathbf{r}}_i(t) = \boldsymbol{\xi}_i(t) + \boldsymbol{\xi}_i^{\text{m}}(t), \quad (131)$$

where the two noise terms are mutually dependent. While equations of this form without the white noise term $\boldsymbol{\xi}_i(t)$ have been frequently used [43–45], the mutual dependence of the two noise terms has not been previously considered. Therefore, this type of equation with

the complicated noise dependency should be explored in future studies. Furthermore, it is necessary to determine whether the mutual dependency of the noises is a general property of the GLE with the mobility kernel.

In addition, another GLE is derived by using a projection operator scheme, and it is shown that the third GLE is consistent with the GLE with the resistance kernel, although there is a subtle difference between the noise terms in the two GLEs. It prompts the question of whether there exists a projection operator scheme consistent with the GLE with the mobility kernel, whose derivation is considerably simpler than that of the GLE with the resistance kernel.

As important examples, the single bead dynamics in the Rouse model and the ring polymer are elucidated using the general framework presented in Sec. IV. In particular, the resistance and mobility kernels for the Rouse model depend on the position i of the tagged bead in the Rouse chain; for example, at long times, the antipersistence in velocity autocorrelation for the end beads is stronger than that for the middle bead [Eq. (108)]. It should be possible to analyze simple polymer models with L being a symmetric circulant matrix and polymerized membranes [39, 46].

A spectral density of states $g(\sigma)$ is the density of the eigenvalues of the Kirchhoff matrix L [5]. For instance, according to Eq. (103), $g(\sigma)$ for the Rouse model is given by $g(\sigma) \sim \sigma^{-1/2}$ as $\sigma \rightarrow 0$. Because $p_{ij}^2 \sim 1$ for small j for the Rouse model, the mobility kernel in Eq. (78) can be expressed as $\gamma\psi(t) \sim -\int g(\sigma)\sigma e^{-\sigma t/\gamma} d\sigma \sim -t^{-3/2}$ in consistent with Eq. (108). Interestingly, various folded proteins have been modeled by the elastic network model, and the spectral density of states for these proteins has been estimated as $g(\sigma) \sim \sigma^\alpha$ with $\alpha \in (0.4, 1.1)$ [5]. Therefore, assuming $p_{ij}^2 \sim 1$ and $\alpha \in (0, 1)$, we obtain $\gamma\psi(t) \sim -t^{-2-\alpha}$. Consequently, the MSD is given by $\langle \mathbf{r}^2(t) \rangle \sim C_1 - C_\alpha t^{-\alpha}$, where C_1 and C_α are positive constants. Thus, the MSD of folded proteins would display power-law relaxation to a plateau at intermediate timescales. These predictions should be verified in future studies (Observing single monomer motion in real proteins is challenging; however, it may be possible in molecular dynamics simulations).

If the interaction matrix L_H can be estimated from experimental or numerical data, it is possible to construct a GLE with a memory kernel, which is determined by L_H [Eq. (129)]. This enables quantitative coarse-grained modeling of complex molecules such as chromatin and proteins. In fact, the estimation of L has been attempted for chromatin using Hi-C data [12, 47] and for proteins using data of their native structures [5]. From the obtained L , the pre-averaged mobility matrix H can be determined analytically or numerically [8, Sec. 4.2]. Thus, we could obtain $L_H = HL$ from experimental data, and this coarse-grained model can be further validated using single-particle-tracking data. Indeed, if trajectory data of single beads in molecules are available from experiments or molecular dynamics simulations, the MSD $\langle \mathbf{r}^2(t) \rangle$ can

be calculated [48]. From the power-law behavior of the MSD at intermediate timescales, the spectral density of states $g(\sigma)$ can be estimated. This information, $g(\sigma)$, should be consistent with the eigenvalue spectrum of the matrix L_H estimated with the structure data.

Hydrodynamic interactions and excluded volume effects are important for describing real polymer systems [8]. The former was incorporated into the present theory using a preaveraging approximation. For the Rouse model, the pre-averaged HI can be further analyzed with normal modes [25], as the preaveraged system is nearly diagonal in the normal modes of the Rouse model without HI [8]. However, it is unclear whether the preaveraged system for the linear elastic model is also nearly diagonal in the normal modes of the original system without HI. Moreover, the excluded volume effects could be incorporated into the present model through a linearization approximation [8], in which the Kirchhoff matrix L (or L_H) should be modified to be consistent with the equilibrium distribution $P_{\text{eq}}(\mathbf{r})$.

Furthermore, recent single-particle-tracking experiments in cells have shown that the diffusion coefficient of tagged particles appears to be random [49–51]. Hydrodynamic interaction is suggested as one of the potential causes of such random diffusivity [52, 53]. However, the preaveraging approximation completely disregards the random fluctuations in diffusivity. Thus, improving the preaveraging approximation to accurately capture the randomly fluctuating diffusivity is crucial for a detailed understanding of experimental data. In addition, the fluctuating diffusivity does not alter the behavior of the mean square displacement, but it does affect higher-order moments such as the non-Gaussian parameter [38, 48, 54]. Therefore, developing data analysis methods to efficiently extract such higher-order information from time series is necessary.

The normal-mode equations of motion in Eqs. (69) and (70) are equivalent to the equations derived in Ref. [32, Eqs. (13) and (14)] from the GLE with the resistance kernel by using a Markovian embedding method. These equations can be utilized for numerical integration of the GLE. Similarly, the normal-mode equations in Eq. (75) can serve as a numerical integration scheme for the GLE with the mobility kernel. They should also provide a means to incorporate fluctuating diffusivity into the GLE in Eq. (131). Incorporating fluctuating diffusivity into such GLEs has been a subject of recent research [45, 51, 55–57], and the normal-mode equations in Eq. (75) offer another approach to achieve this.

In the present paper, only linear models are studied. It would be important for applications to investigate how nonlinear potential forces alter the GLEs [58]. In particular, incorporation of nonlinearity should make the stochastic process non-Gaussian. It might be interesting to attempt deriving a GLE for systems with weak nonlinearity using some perturbation method. If the nonlinearity is sufficiently weak, it should be possible to analytically derive a GLE using the projection operator method

[29]. Furthermore, nonequilibrium dynamics due to the external force $\mathbf{f}_{\text{ex}}(t)$ should also be investigated in future studies [25, 26, 59].

ACKNOWLEDGMENTS

We thank Dr. Takuma Akimoto and Dr. Eiji Yamamoto for fruitful discussion. S.S. was supported by JSPS KAKENHI Grant No. JP23H04297 and JST CREST Grant No. JPMJCR23N3. T.M. was supported by JSPS KAKENHI Grant No. JP22K03436.

Appendix A: Positive definiteness of L'

First, let us assume that L has a zero eigenvalue and $N - 1$ positive eigenvalues. The eigenvector corresponding to the zero eigenvalue is $\mathbf{1}_N = (1, \dots, 1)$. We define an $N \times N$ matrix $L^{(i)}$ as follows. The i th row and column of $L^{(i)}$ are zero, and the other elements are the same as those of L . Then, L and $L^{(i)}$ are congruent; $S^t L S = L^{(i)}$ with a matrix $S := [\mathbf{e}_1, \mathbf{e}_2, \dots, \mathbf{1}_N, \dots, \mathbf{e}_N]$, where \mathbf{e}_j is the N -dimensional unit vector $\mathbf{e}_j := (0, \dots, \overset{(j)}{1}, \dots, 0)$. Thus, due to the Sylvester's law of inertia [34, Sec. 4.5], $L^{(i)}$ has a zero eigenvalue and $N - 1$ positive eigenvalues. It is then evident that the non-zero eigenvalues of the $L^{(i)}$ are equivalent to the eigenvalues of L' . It follows that L' is positive definite.

Appendix B: Proof of $AJ^t JB = AB$

The matrix J defined in Sec. IIIB is explicitly given by

$$J = [\mathbf{e}_1, \dots, \mathbf{e}_{i-1}, \mathbf{e}_N, \mathbf{e}_i, \dots, \mathbf{e}_{N-1}]. \quad (\text{B1})$$

Let \mathbf{a}_j be the j th column vector of A , and \mathbf{b}_j be j th row vector of B . Then, we have

$$AJ^t = [\mathbf{a}_1, \dots, \mathbf{a}_{i-1}, \mathbf{a}_{i+1}, \dots, \mathbf{a}_N, \mathbf{a}_i], \quad (\text{B2})$$

$$JB = [\mathbf{b}_1, \dots, \mathbf{b}_{i-1}, \mathbf{b}_{i+1}, \dots, \mathbf{b}_N, \mathbf{b}_i]^t. \quad (\text{B3})$$

It follows that $AJ^t JB = \sum_{j=1}^N \mathbf{a}_j \mathbf{b}_j = AB$, where each summand $\mathbf{a}_j \mathbf{b}_j$ is an $N \times N$ matrix [34, Sec. 0.2.6].

Appendix C: Numerical scheme

For numerical integration of the Rouse model in Sec. V, the equations of motion are discretized as

$$\gamma [\mathbf{r}(t + dt) - \mathbf{r}(t)] = -\kappa \tilde{L} \cdot \mathbf{r}(t) dt + \sqrt{2\gamma k_B T dt} \tilde{\boldsymbol{\xi}}(t), \quad (\text{C1})$$

where dt is the time step size, \tilde{L} is defined as $\tilde{L} := L/\kappa$ [See Eq. (91)], and $\tilde{\boldsymbol{\xi}}$ is a Gaussian noise with zero mean and unit variance. Note that \tilde{L} and $\tilde{\boldsymbol{\xi}}$ are dimensionless. A discretized velocity $\mathbf{v}_i(t)$ for the tagged particle is defined by

$$\mathbf{v}_i(t) := \frac{\mathbf{r}_i(t + dt) - \mathbf{r}_i(t)}{dt}, \quad (\text{C2})$$

The velocity autocorrelation $\langle \mathbf{v}_i(t) \cdot \mathbf{v}_i(0) \rangle$ is numerically calculated with both time and ensemble averages.

The equation (C1) can be made dimensionless by using transformations

$$\tilde{\mathbf{r}}(\tilde{t}) = \frac{\mathbf{r}(t)}{l_0}, \quad \tilde{t} = \frac{t}{t_0}, \quad (\text{C3})$$

where $l_0 = (k_B T / \kappa)^{1/2}$ and $t_0 = \gamma / \kappa$. In Fig. 2, theoretical and numerical results are presented with these units.

Dimensionless equations of motion for the Rouse model were then given by

$$\tilde{\mathbf{r}}(\tilde{t} + d\tilde{t}) - \tilde{\mathbf{r}}(\tilde{t}) = -\tilde{L} \cdot \tilde{\mathbf{r}}(\tilde{t}) d\tilde{t} + \sqrt{2d\tilde{t}} \tilde{\boldsymbol{\xi}}(\tilde{t}). \quad (\text{C4})$$

As a numerical scheme to integrate Eqs. (C4), the Euler method [60] is used with step size $d\tilde{t} = 0.05$. It is assumed that $\tilde{\mathbf{r}}(0)$ is in equilibrium; the equilibrium distribution is implemented by letting $d\tilde{\mathbf{r}}_m = \tilde{\mathbf{r}}_{m+1}(0) - \tilde{\mathbf{r}}_m(0)$ follow the Gaussian distribution $\propto \exp(-d\tilde{\mathbf{r}}_m^2/2)$ [8].

-
- [1] M. M. Tirion, Large amplitude elastic motions in proteins from a single-parameter, atomic analysis, *Phys. Rev. Lett.* **77**, 1905 (1996).
 - [2] T. Haliloglu, I. Bahar, and B. Erman, Gaussian dynamics of folded proteins, *Phys. Rev. Lett.* **79**, 3090 (1997).
 - [3] I. Bahar, A. R. Atilgan, M. C. Demirel, and B. Erman, Vibrational dynamics of folded proteins: Significance of slow and fast motions in relation to function and stability,

Phys. Rev. Lett. **80**, 2733 (1998).

- [4] A. R. Atilgan, S. Durell, R. L. Jernigan, M. C. Demirel, O. Keskin, and I. Bahar, Anisotropy of fluctuation dynamics of proteins with an elastic network model, *Biophys. J.* **80**, 505 (2001).
- [5] R. Burioni, D. Cassi, F. Cecconi, and A. Vulpiani, Topological thermal instability and length of proteins, *Proteins: Struct. Funct. Genet.* **55**, 529 (2004).

- [6] S. Reuveni, R. Granek, and J. Klafter, Anomalies in the vibrational dynamics of proteins are a consequence of fractal-like structure, *Proc. Natl. Acad. Sci. U.S.A* **107**, 13696 (2010).
- [7] P. E. Rouse, A theory of the linear viscoelastic properties of dilute solutions of coiling polymers, *J. Chem. Phys.* **21**, 1272 (1953).
- [8] M. Doi and S. F. Edwards, *The Theory of Polymer Dynamics* (Oxford University Press, Oxford, 1986).
- [9] G. Le Treut, F. Képès, and H. Orland, A polymer model for the quantitative reconstruction of chromosome architecture from HiC and GAM data, *Biophysical journal* **115**, 2286 (2018).
- [10] L. Liu, M. H. Kim, and C. Hyeon, Heterogeneous loop model to infer 3D chromosome structures from Hi-C, *Biophys. J.* **117**, 613 (2019).
- [11] G. Shi and D. Thirumalai, Conformational heterogeneity in human interphase chromosome organization reconciles the FISH and Hi-C paradox, *Nat. Commun.* **10**, 3894 (2019).
- [12] S. Shinkai, M. Nakagawa, T. Sugawara, Y. Togashi, H. Ochiai, R. Nakato, Y. Taniguchi, and S. Onami, PHIC: deciphering Hi-C data into polymer dynamics, *NAR Genomics Bioinforma* **2**, lqaa020 (2020).
- [13] I. Bronstein, Y. Israel, E. Kepten, S. Mai, Y. Shav-Tal, E. Barkai, and Y. Garini, Transient anomalous diffusion of telomeres in the nucleus of mammalian cells, *Phys. Rev. Lett.* **103**, 018102 (2009).
- [14] S. C. Weber, A. J. Spakowitz, and J. A. Theriot, Bacterial chromosomal loci move subdiffusively through a viscoelastic cytoplasm, *Phys. Rev. Lett.* **104**, 238102 (2010).
- [15] S. Hihara, C.-G. Pack, K. Kaizu, T. Tani, T. Hanafusa, T. Nozaki, S. Takemoto, T. Yoshimi, H. Yokota, N. Imamoto, *et al.*, Local nucleosome dynamics facilitate chromatin accessibility in living mammalian cells, *Cell Rep.* **2**, 1645 (2012).
- [16] S. Shinkai, T. Nozaki, K. Maeshima, and Y. Togashi, Dynamic nucleosome movement provides structural information of topological chromatin domains in living human cells, *PLOS Comp. Biol.* **12**, e1005136 (2016).
- [17] H. Ohishi, S. Shimada, S. Uchino, J. Li, Y. Sato, M. Shintani, H. Owada, Y. Ohkawa, A. Pertsinidis, T. Yamamoto, *et al.*, Streaming-tag system reveals spatiotemporal relationships between transcriptional regulatory factors and transcriptional activity, *Nat. Commun.* **13**, 7672 (2022).
- [18] T. Nozaki, S. Shinkai, S. Ide, K. Higashi, S. Tamura, M. A. Shimazoe, M. Nakagawa, Y. Suzuki, Y. Okada, M. Sasai, S. Onami, K. Kurokawa, S. Iida, and K. Maeshima, Condensed but liquid-like domain organization of active chromatin regions in living human cells, *Sci. Adv.* **9**, eadf1488 (2023).
- [19] S. C. Kou and X. S. Xie, Generalized Langevin equation with fractional gaussian noise: Subdiffusion within a single protein molecule, *Phys. Rev. Lett.* **93**, 180603 (2004).
- [20] W. Min, G. Luo, B. J. Cherayil, S. C. Kou, and X. S. Xie, Observation of a power-law memory kernel for fluctuations within a single protein molecule, *Phys. Rev. Lett.* **94**, 198302 (2005).
- [21] D. Panja, Generalized Langevin equation formulation for anomalous polymer dynamics, *J. Stat. Mech.* **2010**, L02001 (2010).
- [22] D. Panja, Anomalous polymer dynamics is non-Markovian: memory effects and the generalized Langevin equation formulation, *J. Stat. Mech.* **2010**, P06011 (2010).
- [23] L. Lizana, T. Ambjörnsson, A. Taloni, E. Barkai, and M. A. Lomholt, Foundation of fractional Langevin equation: Harmonization of a many-body problem, *Phys. Rev. E* **81**, 051118 (2010).
- [24] H. Vandebroek and C. Vanderzande, On the generalized Langevin equation for a Rouse bead in a nonequilibrium bath, *J. Stat. Phys.* **167**, 14 (2017).
- [25] T. Sakaue, Memory effect and fluctuating anomalous dynamics of a tagged monomer, *Phys. Rev. E* **87**, 040601(R) (2013).
- [26] T. Saito and T. Sakaue, Driven anomalous diffusion: An example from polymer stretching, *Phys. Rev. E* **92**, 012601 (2015).
- [27] X. Tian, X. Xu, Y. Chen, J. Chen, and W.-S. Xu, Explicit analytical form for memory kernel in the generalized Langevin equation for end-to-end vector of Rouse chains, *J. Chem. Phys.* **157**, 224901 (2022).
- [28] J.-P. Hansen and I. R. McDonald, *Theory of Simple Liquids* (Elsevier, New York, 1990).
- [29] J. K. G. Dhont, *An Introduction to Dynamics of Colloids* (Elsevier, Amsterdam, 1996).
- [30] T. Yuan, H. Yan, M. L. P. Bailey, J. F. Williams, I. Surovtsev, M. C. King, and S. G. J. Mochrie, Effect of loops on the mean-square displacement of Rouse-model chromatin, *Phys. Rev. E* **109**, 044502 (2024).
- [31] R. Kubo, M. Toda, and N. Hashitume, *Statistical Physics II. Nonequilibrium Statistical Mechanics* (Springer-Verlag, 1991).
- [32] T. Miyaguchi, Generalized langevin equation with fluctuating diffusivity, *Phys. Rev. Res.* **4**, 043062 (2022).
- [33] N. Pottier, Aging properties of an anomalously diffusing particle, *Physica A* **317**, 371 (2003).
- [34] R. A. Horn and C. R. Johnson, *Matrix Analysis* (Cambridge University Press, New York, 2012).
- [35] D. J Evans and G. P Morriss, *Statistical Mechanics of Nonequilibrium Liquids* (Cambridge University Press, Cambridge, 2008).
- [36] W. Feller, *An Introduction to Probability Theory and its Applications*, 3rd ed., Vol. I (Wiley, New York, 1968).
- [37] A. Amitai and D. Holcman, Polymer model with long-range interactions: Analysis and applications to the chromatin structure, *Phys. Rev. E* **88**, 052604 (2013).
- [38] T. Miyaguchi, T. Uneyama, and T. Akimoto, Brownian motion with alternately fluctuating diffusivity: Stretched-exponential and power-law relaxation, *Phys. Rev. E* **100**, 012116 (2019).
- [39] R. Keesman, G. T. Barkema, and D. Panja, Dynamical eigenmodes of a polymerized membrane, *J. Stat. Mech.* **2013**, P04009 (2013).
- [40] T. H. Berlin and M. Kac, The spherical model of a ferromagnet, *Phys. Rev.* **86**, 821 (1952).
- [41] E. Yamamoto, T. Akimoto, Y. Hirano, M. Yasui, and K. Yasuoka, $1/f$ fluctuations of amino acids regulate water transportation in aquaporin 1, *Phys. Rev. E* **89**, 022718 (2014).
- [42] M. F. Thorpe, Comment on elastic network models and proteins, *Phys. Biol.* **4**, 60 (2007).
- [43] W. Deng and E. Barkai, Ergodic properties of fractional Brownian-Langevin motion, *Phys. Rev. E* **79**, 011112 (2009).
- [44] J. Kursawe, J. Schulz, and R. Metzler, Transient aging in fractional Brownian and Langevin-equation motion,

- Phys. Rev. E **88**, 062124 (2013).
- [45] J. Janczura, M. Balcerek, K. Burnecki, A. Sabri, M. Weiss, and D. Krapf, Identifying heterogeneous diffusion states in the cytoplasm by a hidden Markov model, *New J. Phys.* **23**, 053018 (2021).
 - [46] K. Mizuochi, H. Nakanishi, and T. Sakaue, Dynamical scaling of polymerized membranes, *Europhys. Lett.* **107**, 38003 (2014).
 - [47] S. Shinkai, H. Itoga, K. Kyoda, and S. Onami, PHi-C2: interpreting Hi-C data as the dynamic 3D genome state, *Bioinformatics* **38**, 4984 (2022).
 - [48] T. Uneyama, T. Miyaguchi, and T. Akimoto, Fluctuation analysis of time-averaged mean-square displacement for the Langevin equation with time-dependent and fluctuating diffusivity, *Phys. Rev. E* **92**, 032140 (2015).
 - [49] B. R. Parry, I. V. Surovtsev, M. T. Cabeen, C. S. O'Hern, E. R. Dufresne, and C. Jacobs-Wagner, The bacterial cytoplasm has glass-like properties and is fluidized by metabolic activity, *Cell* **156**, 183 (2014).
 - [50] T. J. Lampo, S. Stylianidou, M. P. Backlund, P. A. Wiggins, and A. J. Spakowitz, Cytoplasmic RNA-protein particles exhibit non-Gaussian subdiffusive behavior, *Biophys. J.* **112**, 532 (2017).
 - [51] A. Sabri, X. Xu, D. Krapf, and M. Weiss, Elucidating the origin of heterogeneous anomalous diffusion in the cytoplasm of mammalian cells, *Phys. Rev. Lett.* **125**, 058101 (2020).
 - [52] T. Miyaguchi, Elucidating fluctuating diffusivity in center-of-mass motion of polymer models with time-averaged mean-square-displacement tensor, *Phys. Rev. E* **96**, 042501 (2017).
 - [53] E. Yamamoto, T. Akimoto, A. Mitsutake, and R. Metzler, Universal relation between instantaneous diffusivity and radius of gyration of proteins in aqueous solution, *Phys. Rev. Lett.* **126**, 128101 (2021).
 - [54] T. Uneyama, T. Miyaguchi, and T. Akimoto, Relaxation functions of the Ornstein-Uhlenbeck process with fluctuating diffusivity, *Phys. Rev. E* **99**, 032127 (2019).
 - [55] W. Wang, F. Seno, I. M. Sokolov, A. V. Chechkin, and R. Metzler, Unexpected crossovers in correlated random-diffusivity processes, *New J. Phys.* **22**, 083041 (2020).
 - [56] W. Wang, A. G. Cherstvy, A. V. Chechkin, S. Thapa, F. Seno, X. Liu, and R. Metzler, Fractional Brownian motion with random diffusivity: emerging residual non-ergodicity below the correlation time, *J. Phys. A* **53**, 474001 (2020).
 - [57] C. Dieball, D. Krapf, M. Weiss, and A. Godec, Scattering fingerprints of two-state dynamics, *New J. Phys.* **24**, 023004 (2022).
 - [58] S. Milster, F. Koch, C. Widder, T. Schilling, and J. Dzubiella, Tracer dynamics in polymer networks: Generalized Langevin description, *The Journal of Chemical Physics* **160**, 094901 (2024).
 - [59] B. Cui and A. Zacccone, Generalized Langevin equation and fluctuation-dissipation theorem for particle-bath systems in external oscillating fields, *Phys. Rev. E* **97**, 060102(R) (2018).
 - [60] P. E. Kloeden and E. Platen, *Numerical Solution of Stochastic Differential Equations* (Springer, Berlin, 2011).